Differences in removal rates of virgin/decayed microplastics, viruses, activated carbon, and kaolin/montmorillonite clay particles by coagulation, flocculation, sedimentation, and rapid sand filtration during water treatment

Yoshifumi Nakazawa [a], Taketo Abe [b], Yoshihiko Matsui [c,*], Koki Shinno [b], Sakiko Kobayashi [b], Nobutaka Shirasaki [c], Taku Matsushita [c]

[a] *Department of Environmental Health, National Institute of Public Health, 2-3-6 Minami, Wako, Saitama, 351-0197, Japan*

[b] *Graduate School of Engineering, Hokkaido University, N13W8, Sapporo 060-8628, Japan*

[c] *Faculty of Engineering, Hokkaido University, N13W8, Sapporo 060-8628, Japan*

* Corresponding author: Yoshihiko Matsui, Faculty of Engineering, Hokkaido University, N13W8, Sapporo 060-8628, Japan

E-mail address: matsui@eng.hokudai.ac.jp (Y. Matsui)

Tel./fax: +81-11-706-7280

Abstract

One of the main purposes of drinking water treatment is to reduce turbidity originating from clay particles. Relatively little is known about the removal of other types of particles, including conventionally sized powdered activated carbon (PAC) and superfine PAC (SPAC), which are intentionally added during the treatment process; microplastic particles; and viruses. To address this knowledge gap, we conducted a preliminary investigation in full-scale water treatment plants and then studied the removal of these particles during coagulation-flocculation, sedimentation, and rapid sand filtration (CSF) in bench-scale experiments in which these particles were present together. Numbers of all target particles were greatly decreased by coagulation-flocculation and sedimentation (CS). Subsequent rapid sand filtration greatly reduced the concentrations of PAC and SPAC but not the concentrations of viruses, microplastic particles, and clay particles. Overall removal rates by CSF were 4.6 logs for PAC and SPAC, 3.5 logs for viruses, 2.9 logs for microplastics, and 2.8 logs for clay. The differences in removals were not explained by particle sizes or zeta potentials. However, for clays, PAC and SPAC, for which the particle size distributions were wide, smaller particles were less efficiently removed. The ratios of both clay to PAC and clay to SPAC particles increased greatly after rapid sand filtration because removal rates of PAC and SPAC particles were about 2 logs higher than removal rates of clay particles. The trend of greater reduction of PAC concentrations than turbidity was confirmed by measurements made in 14 full-scale water purification plants in which residual concentrations of PAC in treated water were very low, 40–200 particles/mL. Clay particles therefore accounted for most of the turbidity in sand filtrate, even though PAC was employed. The removal rate of microplastic particles was comparable to that of clays. Sufficient turbidity removal would therefore provide comparable removal of microplastics. We investigated the effect of mechanical/photochemical weathering on the removal of microplastics via CSF. Photochemical weathering caused a small increment in the removal rate

of microplastics during CS but a small reduction in the removal rate of microplastics during rapid sand filtration; mechanical weathering decreased the removal rate via CS but increased the removal rate via rapid sand filtration. The changes of removal of microplastics might have been caused by changes of their zeta potential.

Keywords: Log-removal, Number concentrations, MS2, PMMoV, Weathering

53 Abbreviations

Shortened word	Meaning
AC	activated carbon
PAC	powdered activated carbon
SPAC	superfine powdered activated carbon
GAC	granular activated carbon
MP	microplastic
PA	polyamide
PA-pw	photochemically weathered PA
PA-md	mechanically damaged PA
PSi	polysilicone
PE	polyethylene
PMMoV	pepper mild mottle virus
PACl	poly-aluminum chloride
CSF	coagulation-flocculation, sedimentation, and rapid sand filtration
CS	coagulation-flocculation and sedimentation
PCR	polymerase chain reaction
ZP	zeta potential
D50	volume median diameter
FTIR	Fourier transform infrared spectroscopy
UV	ultraviolet
VUV	vacuum ultraviolet

54

55

1. Introduction

The primary objective of drinking water treatment via coagulation-flocculation, sedimentation, and rapid sand filtration (CSF) is to reduce turbidity by removing suspended solids, which consist primarily of clay particles. Turbidity reduction via CSF has been thoroughly studied (Edzwald 2011). CSF has proven effective in removing clay particles (WHO 2019), but the behavior of particles in CSF and the residual of low concentrations of suspended solids in sand filtrate have not been adequately discussed. The sensitivity of turbidity measurements is insufficient to evaluate trace concentrations of particles and their high removal rates (log reduction) (Cho *et al.* 2020). In contrast, the removal of viruses (particle sizes: 30–100 nm) via CSF has been studied by quantifying their number concentrations with results using the real-time polymerase chain reaction (PCR), and removals of 0.8−2.5 log levels via normal CSF operations have been reported (Asami *et al.* 2016, Kato *et al.* 2018, Shirasaki *et al.* 2018). Activated carbon (AC) particles, which are usually dosed before coagulation and are expected to be removed by CSF, are black in color; however, if they remain in treated water, they tend to be conspicuous and cause consumer dissatisfaction. There is hence a need to reduce the concentrations of AC particles to extremely low levels that would have no detectable effect on turbidity. Our research group has also examined the removability of AC particles (particle sizes 1.0−14 μm) by counting the numbers of carbon particles under a microscope (Nakazawa *et al.* 2018).

Recently, microplastic (MP) particles have drawn attention throughout the world because they have been found to be widely distributed in the ocean, freshwater, air, and soil (Dris *et al.* 2016, Freeman *et al.* 2020, Iqbal *et al.* 2020, Iwasaki *et al.* 2017, Koelmans *et al.* 2019, Rodrigues *et al.* 2018, Uurasjärvi *et al.* 2020, Wang *et al.* 2021, Wong *et al.* 2020, Wu *et al.* 2019, Zhou *et al.* 2020). Because MPs <10 μm in size have been reported to adversely affect human health (Kögel *et al.* 2020, Revel *et al.* 2018), their fate in drinking water treatment should

be well understood (Syberg *et al.* 2015, WHO 2019). Among available drinking water treatment processes, membrane filtration can separate MPs entirely (Ma *et al.* 2019). However, CSF is still the major water treatment process in Japan and other countries, and there is concern that MPs may pass through CSF treatment systems and enter the distribution system because particles are probabilistically separated and removed in CSFs.

MPs have actually been detected in treated water as well as raw water of some full-scale water treatment plants (Kosuth *et al.* 2018, Mintenig *et al.* 2019, Pivokonsky *et al.* 2018, Shen *et al.* 2020, Wang *et al.* 2020b). Whereas MPs are present in treated groundwater in extremely low concentrations (0−1 particles/m^3) (Mintenig et al. 2019), the MP concentrations in treated river water are much higher. When river water has been treated by coagulation, floatation, sand filtration, and passage through granular activated carbon (GAC), the residual MP concentration in the finished water has been 628 particles/L, which is slightly lower than the concentration associated with ecological risks (Elizalde-Velázquez and Gómez-Oliván 2021), and the percent removal of MPs has been 83% (Pivokonsky et al. 2018). The detected MPs had shapes like fragments and fibers, and most of them were <10 μm in size. Wang et al. (2020b) have investigated a water treatment plant (CSF and ozonation combined with GAC filtration) and have reported a similar concentration and removal rate of MPs.

Quite recently, the effects of water treatment conditions on the treatability of MPs have been investigated by using waters spiked with MPs (Ma et al. 2019, Rajala *et al.* 2020, Skaf *et al.* 2020, Wang *et al.* 2020c, Zhou *et al.* 2021). However, those studies have used water spiked with MPs at unrealistically high concentrations. There is a need to evaluate removal performances with trace MP concentrations that reflect actual levels of contamination. In addition, some studies have used fluorescent MPs that have larger specific gravities than naked MPs (Skaf et al. 2020), but the changes due to fluorescent marking of the physical properties of the MPs (Zhou et al. 2021), including their specific gravities, may have affected the removal

efficiencies. Zhang *et al.* (2020) have used fluorescent particles at concentrations similar to those observed in river water (1800−9500 particles/L) and have reported removal rates of 86.9−99.9%. However, Zhang et al. (2020) used a filter that consisted of cheesecloth and anthracite, which is not widely used in water treatment compared with a sand filter composed of quartz sand. Moreover, it has been reported that industrially produced MPs are mechanically/photochemically weathered after being emitted to the environment (Sun *et al.* 2020), and the hydrophobicity and chemical composition of weathered MPs (WHO 2019) differ from those of MPs prior to weathering (Lin *et al.* 2020, Naik *et al.* 2020, Wang *et al.* 2020a, Zhu *et al.* 2020a, Zhu *et al.* 2020b). The changes related to weathering of MPs might affect the efficiency of their removal in water treatment.

Collectively, the above-mentioned studies suggest that the removal rates of particles that contaminate raw water to be treated for drinking purposes may differ greatly as a function of the type of particles: ~1 log removal for MPs 0.2 −100 μm in size (Zhang et al. 2020), 0.8−2.5 log removal for viruses in the size range 30−100 nm (Asami et al. 2016, Kato et al. 2018, Shirasaki et al. 2018), and 5−6 log removal for AC particles 1.0−14 μm in size (Nakazawa et al. 2018).

However, these removal rates vary as a function of treatment conditions, and no studies have compared the removal rates of various types of particles in a mixture of particle types. Moreover, no information of log particle removal is available for clay causing turbidity, although the efficiency of removal of clay may be roughly inferred from changes of turbidity, and there have been no comparisons of the removal efficiencies of particles of all sizes by CSF under the same conditions and at concentrations representative of those encountered in the treatment of public water supplies. For example, even the basic question of whether MPs and viruses are more easily removed than clay particles has not been answered.

130 Accordingly, the objective of the present study was to determine the fates and removal
131 efficiencies of MPs, clay, AC, and virus particles during CSF. Clay, AC, and viruses are
132 conventional targets of CSF removal, and MPs are emerging targets of micropollutant removal.
133 Our application of counting methods to identify and quantify clay and AC particles as well as
134 MP particles enabled us to carry out the first comparative analysis of their removal by CSF
135 based on the number concentrations of all particles, including viruses.
136
137 **2. Materials and methods**
138
139 *2.1. Target particles*
140
141 *2.1.1. MPs*
142 Microspheres of nylon composed of polyamides (NYLON 12, SP-500; D50 (volume median
143 diameter), 4.8 μm; density = 1.02 g cm^{-3}; hereafter 'PA') were provided by Toray Industries,
144 Inc. (Tokyo, Japan). Polysilicone microspheres (KMP-600; D50, 4.8 μm; 0.99 g cm^{-3}; hereafter
145 'PSi') were provided by Shin-Etsu Chemical Co., Ltd. (Tokyo, Japan). Polyethylene
146 microspheres (LE-1080; D50, 6.5 μm; 0.92 g cm^{-3}; hereafter 'PE') were provided by Sumitomo
147 Seika Chemicals Company, Ltd. (Osaka, Japan).
148 Before their use in experiments, these MPs were prepared as suspensions via the following
149 procedure. First, each type of MP was added to pure water (Milli-Q water; Milli-Q Advantage
150 A10 System; Merck KGaA, Darmstadt, Germany) at a concentration of 100 mg/L. To
151 sufficiently disperse the MPs in the water, the MP suspension was exposed to ultrasonic
152 treatment (FU-180C, Tokyo Garasu Kikai Co., Ltd., Tokyo, Japan) for 24 h and then stored at
153 4 °C before use. Before raw water was prepared for the CSF tests, the MP suspension was
154 diluted with Milli-Q water to a concentration of 23.2 μg/L and then exposed to ultrasonic

155 treatment (CPX8800h-J, Yamato Scientific Co., Ltd., Tokyo, Japan) for 30 min. Before
156 measuring the and zeta potential (ZP) (see also Section 2.7), the MP suspension was exposed
157 to ultrasonic sound waves (CPX8800h-J) for 30 min and diluted appropriately for the
158 measurements.

159 Photochemical weathering was simulated on PA as follows. First, a PA suspension was
160 prepared by addition of PA to Milli-Q water contained in a clear glass bottle at a concentration
161 of 50 mg/L and then exposed to ultrasonic treatment (FU-180C, Tokyo Garasu Kikai Co., Ltd.)
162 for 24 h. The bottle containing the PA suspension was then placed by a window and inverted
163 each day to expose the PAs to sunlight for 68 days from 18 August to 24 October 2020.
164 Henceforth, this photochemically weathered PA is denoted as PA-pw.

165 Mechanical weathering of PA was simulated as follows. First, PA (10 g) was transferred to
166 a closed-chamber, ball-mill pot that contained 5- and 10-mm-diameter Al_2O_3 balls as the
167 disintegrating medium. After the pot had been rotated at 94 rpm for 24 h, the PA was retrieved.
168 This mechanically damaged PA is henceforth denoted as PA-md.

169

170 *2.2.2. Activated carbon*

171 Conventionally sized PAC (hereafter PAC; D50, 14 μm) and superfine PAC (SPAC; D50, 0.81
172 μm) were used as target ACs. The PAC was a commercially available, wood-based PAC (Taiko
173 W; Futamura Chemical Co., Ltd., Nagoya, Japan). SPAC was prepared from the PAC by wet-
174 mode ball milling (Nikkato, Osaka, Japan) followed by wet-mode bead milling (LMZ015;
175 Ashizawa Finetech, Ltd., Chiba, Japan) in our laboratory. Details of the preparation procedure
176 have been reported previously (Pan *et al.* 2017). Determination of the volume median diameter
177 (D50) is described in Section 2.7.

178

179 *2.2.3. Clay*

180 Commercially available kaolin (D50, 5.6 μm; FUJIFILM Wako Pure Chemical Corp., Osaka,
181 Japan) and montmorillonite (D50, 12 μm; Sigma-Aldrich Co., LLC., St. Louis, MO, USA) were
182 used as the targets for clay removal. Kaolin and montmorillonite are the major clay minerals in
183 most soils (Adamis and Williams 2005). These clay minerals were added to Milli-Q water at 10
184 g L^{-1} to prepare stock suspensions. D50 determination is described in Section 2.7.
185
186 *2.2.4. Viruses*
187 F-specific RNA bacteriophage MS2 [diameter, 0.026 μm (Shirasaki *et al.* 2017); NBRC 102619,
188 National Institute of Technology and Evaluation Biological Research Center, Kisarazu, Japan]
189 and pepper mild mottle viruses [rod-shaped particles with diameter 0.018 × length 0.3 μm
190 (Shirasaki et al. 2017); PMMoV pepIwateHachiman1 strain, MAFF 104099, National Institute
191 of Agrobiological Sciences Genebank, Tsukuba, Japan] were used as the targets for virus
192 removal after being propagated in *Escherichia coli* bacterial hosts (NBRC 13965) and
193 *Nicotiana benthamiana*, respectively, followed by purification. The concentrations were
194 quantified by the real-time polymerase chain reaction (PCR). Details of the procedures for the
195 propagation, purification, and quantification of the viruses have been described previously
196 (Shirasaki *et al.* 2016, Shirasaki et al. 2018).
197
198 *2.3. Coagulant*
199
200 Commercially available, conventional poly-aluminum chloride [PACl; basicity of 1.5
201 (basicity of 50%), sulfate ion 2.9 wt%], provided by Taki Chemical Co., Ltd. (Hyogo, Japan),
202 was used as a coagulant.
203
204 *2.4. Bench-scale CSF tests*

Water taken from the Toyohira River (Table S1 for water quality) at the Moiwa Water Purification Plant (Sapporo, Japan; sampled on 24 June 2020) was filtered through a membrane filter (pore diameter 0.2 mm; PTFE; Toyo Roshi Kaisha, Ltd., Tokyo, Japan) to remove suspended matter. For the CSF tests, this filtered water was supplemented with stock suspensions of PAC (10 mg/L, 7−8 NTU, 4.0×10^6 particles/mL), SPAC (2.0 mg/L, 7−8 NTU, 5.1×10^6 particles/mL), MP (1.0 μg/L, 11 particles/mL), viruses (10^7 copies/mL), and/or clay particles (10 mg/L, 7−8 NTU, 8.7×10^5 particles/mL, for kaolin; 10 mg/L, 1.8 NTU, 2.2×10^4 particles/mL, for montmorillonite). The concentrations of clay and AC particles were comparable to the concentrations that might be found in typical raw water. Because we assumed that MPs and viruses were present at low concentrations in river water, their concentrations were set to be as low as possible for measurement. The theoretical increase of dissolved organic carbon (DOC) by the addition of the virus stock was 0.05 mg-C/L, which was much smaller than the DOC of water from the Toyohira River (0.8 mg/L). We therefore assumed that the addition of MPs and viruses had little effect on the removal of other particles. We prepared 17 kinds of water (Table S2), each of which contained either kaolin or montmorillonite, either PAC or SPAC, and one kind of MP. Two of the 17 raw waters contained viruses in addition to PAC, kaolin, and PE particles. The removal rates of the different kinds of particles were compared in water subject to the same CSF.

The CSF test was conducted in a rectangular beaker containing 11 L of raw water (Fig. S1). The dosage of the coagulant PACl was predetermined to be 3.0 mg-Al/L (unless otherwise noted). Under these conditions, visible floc particles were formed, and the turbidity of the supernatant after 60 min of sedimentation was < 0.2 NTU. The coagulant was injected into the raw water after adding NaOH to bring the coagulation pH to 7.0. Rapid mixing for coagulation was conducted at a G value of 600 s^{-1} for 100 s and was followed by slow mixing for

230 flocculation at a G value of 12.5 s^{-1} for 2400 s. After the slow mixing, the water was allowed
231 to remain quiescent for 60 min to allow sedimentation to proceed. Virus concentrations in the
232 supernatant were determined directly without further treatment. A portion of the supernatant
233 was subjected to centrifugation pretreatment or ultrasonication pretreatment before
234 determination of the concentrations of AC, MP, and clay particles (see Section 2.6). Ten liters
235 of the sedimentation supernatant was transferred to another beaker, and the supernatant in the
236 beaker was pumped to a sand filter (effective diameter and uniformity of sand grains: 0.94 mm
237 and 1.24, sand depth 50 cm, column inner diameter 3.6 cm). Rapid sand filtration was performed
238 in the down-flow direction at a rate of 90 m d^{-1}. The sand filtrate was collected from 0 to 50
239 min to determine the turbidity and concentration of each kind of particle. After each filtration
240 run, the sand filter was backwashed with tap water and then forward washed with Milli-Q water.
241 After each test, instruments that had contacted viruses were exposed to chlorine and washed
242 with Milli-Q water to prevent viral contamination during the next run.
243
244 *2.5. Centrifugation and ultrasonication pretreatments*
245
246 A portion of the supernatant from the sedimentation was pretreated by centrifugation to
247 determine the concentrations of stray, un-flocculated AC and clay particles that were not
248 incorporated into floc particles. Aliquots (45 mL) of a supernatant sample collected after
249 sedimentation were dispensed into four 50-mL glass tubes. The tubes were centrifuged (CT6E;
250 Koki Holdings Co., Ltd., Tokyo, Japan) in a swing rotor (T5SS; Koki Holdings Co., Ltd.) at
251 3990 *g* for 10 min, halted for 2 min, and then re-centrifuged for 10 min (Nakazawa *et al.* 2021).
252 The concentrations of particles in the centrifugal supernatant were then determined by
253 membrane filtration and microscopic image analysis (see Section 2.6).

254 Ultrasonication pretreatment was used to disperse and determine the concentrations of AC,
255 clay, and MP particles in the supernatant. The supernatant sample collected after sedimentation
256 was transferred to a glass bottle, and HCl was added to bring the pH to < 3. The resultant water
257 was exposed to ultrasonic treatment (CPX8800h-J, Yamato Scientific Co., Ltd.) for 1 h to
258 disperse particles suspended in the water. The concentrations of particles in the sonicated water
259 were then determined by membrane filtration and microscopic image analysis (see Section 2.6).
260
261 *2.6. Measurement of particle concentrations*
262
263 MP, AC, and clay particles in each water sample were captured by filtering the water
264 through a white membrane filter (nominal pore diameter, 0.1 μm; membrane diameter 25 mm;
265 polytetrafluoroethylene; Merck KGaA, Darmstadt, Germany) and, separately, through a black
266 membrane filter (nominal pore diameter, 0.45 μm; membrane diameter 25 mm; mixed cellulose
267 esters; Merck KGaA). The filters were dried at room temperature.
268 AC particles were detected on color photomicrographs taken of the surface of the white
269 membrane filter by a digital microscope (VHX-2000; Keyence Corp., Osaka, Japan) at 1000×
270 magnification by using the image analysis software associated with the microscope, and then
271 their particle number concentration and particle size were calculated. MP particles were
272 detected on the color photomicrographs taken of the surface of the white membrane filter at
273 500× magnification and quantified. Clay particles were detected on the surface of the black
274 membrane filter at 1000× magnification and quantified. The minimum sizes of detectable
275 particles were 0.23 μm at 1000× magnification and 0.47 μm at 500× magnification.
276 Virgin MP particles (spherical) and clay particles (non-spherical) in the same
277 photomicrographs were identified and detected separately based on their shape. However,

because most PA-md particles were non-spherical, no CSF test using the mixture of PA-md and clay particles was conducted.

2.7. Other analysis of particles

Determination of the D50s of MP, AC, and clay particles in a completely dispersed form was carried out using a laser-light-diffraction and scattering method (Microtrac MT3300EXII; MicrotracBEL Corp., Osaka, Japan) after adding a dispersant (Triton X-100; Kanto Chemical Co., Inc., Tokyo, Japan; final concentration, 0.08% w/v) and exposing a 50-mL particle suspension to ultrasonication (US-300E; Nihonseiki Kaisha Ltd., Tokyo, Japan) for 1 min (Fig. S2 and Table 1).

The ZPs of AC, MP, and clay particles as functions of pH were determined as follows. Filtered water from the Toyohira River (Sapporo) was supplemented with a stock suspension of PAC (10 mg/L), SPAC (2.0 mg/L), MP (1.0 mg/L), or clay particles (10 mg/L). Either NaOH or HCl was added to the resulting water to adjust the pH to a value in the range 1.5−11.5, and the ZP was measured (Zetasizer Nano ZS; Malvern, United Kingdom).

Fourier transform infrared spectroscopy (FTIR) analysis of MPs was conducted with an FTIR spectrophotometer (IR-7500S, Shimadzu, Kyoto, Japan) at a resolution of 4 cm^{-1} (Ninomiya *et al.* 2020) with KBr pellets containing PA or PA-pw particles at 0.25 wt%.

PA, PA-pw, and PA-md particles were collected on a membrane filter (nominal pore diameter, 0.45 μm; diameter 25 mm; mixed cellulose esters; Merck KGaA). The particles on the filter were observed using a field-emission scanning electron microscope (JSM-7400F, JEOL, Ltd., Tokyo, Japan).

Table 1

Diameters and zeta potentials of particles.

particle	Volume median diameter (D50)	ZP at pH 7
	μm	mV
PAC	14	−23
SPAC	0.81	−20
kaolin	5.6	−24
montmorillonite	12	−18
PA	4.8	−19
PA−pw	4.9	−16
PA−md	5.0	−22
PE	6.5	−15
PSi	4.8	−16
PMMoV	diameter 0.018, length 0.3[a] (rod-shaped particle)	−26[b]
MS2	diameter 0.026[a] (spherical particle)	−51[c]

[a] Shirasaki et al. (2017).

[b] Calculated by using Henry equation with an electrophoretic mobility (Shirasaki et al. 2017).

[c] Calculated by using Henry equation with an electrophoretic mobility (Shirasaki et al. 2016).

2.8. Sampling of sand filtrates in full-scale water purification plants

Sampling of sand filtrates was conducted at 14 full-scale water-treatment plants in Japan that used the CSF process (Table S3) and were using PAC to treat the water. The samples were quantified for residual black-particle concentrations by using membrane filtration and microscopic image analysis as described in Section 2.6.

3. Results and Discussion

320 *3.1. Residual carbon particles in full-scale CSF plants*

321

322 Fig. 1 shows the residual concentrations of carbon particles in sand filtrates in the 14 full-
323 scale water purification plants that treated their raw water by adding PAC followed by the CSF
324 process. The residual concentrations of carbon particles were plotted against the PAC dosages,
325 but there was little correlation (R^2=0.13, Fig. 1). This result was reasonable because plant
326 configurations and operations differed. There was a weak correlation between the residual
327 concentrations of carbon particle and the turbidities of the sedimentation supernatants (R^2=0.44,
328 Fig. S3, Supplementary Information [SI]). The concentrations of residual carbon particles in
329 sand filtrates were in the range 40–200 particles/mL (n.b., There were no reports of customer
330 complaints about black particles in the waters supplied from these plants.). The highest
331 concentration (200 particles/mL) with no customer complaints could be considered a rough
332 indication for the goal of treatment with SPAC, which is not used in conventional water
333 treatment consisting of CSF because of concern over its leakage. Turbidities of the sand filtrates
334 were not different from those observed when the same plants were operated without PAC
335 addition (data not shown).

336 There was no correlation between the turbidities and concentrations of PAC particles in
337 sand filtrates (Fig. S4). The PAC particles were removed more efficiently than the usual
338 turbidity components, most of which were probably clay particles. The turbidity of the raw
339 water before the addition of PAC was 1.9−18 NTU; the turbidity removal rates were estimated
340 to be in the range of 1–4 logs when calculated from the turbidity of the water after CSF treatment.
341 PAC removals by the CSFs were 3.4−4.9 logs (4.2±0.4 logs, average±SD) in terms of particle
342 number concentrations (Fig. S5). Consequently, the hypothetical turbidity originating from the
343 PAC particles in sand filtrates, that was estimated to be 4.7×10^{-6} to 6.7×10^{-5} NTU (Kissa
344 1999, Nakazawa et al. 2018), was much smaller than the observed turbidity. Therefore, not only

345 do the concentrations of suspended particles vary greatly depending on the particle type, such
346 as clay or PAC, but also their removal rates are likely to vary greatly. As a result, the observed
347 turbidity could be unrelated to the concentrations of other type of particles, such as PAC
348 particles.

349 On the other hand, the turbidity data could not be used to exactly compare the removals of
350 turbidity components (clay particles) with AC particles because the principles associated with
351 quantification of turbidity are quite different from those associated with quantification of
352 particle counts. Also, the limit of quantification of turbidity is insufficient to accurately estimate
353 log removals: e.g., a log removal > 3 is hard to estimate precisely when the initial turbidity is
354 10 NTU and the turbidity quantification limit is 0.01, which is a typical value. The bench-scale
355 experimental testing in the subsequent sections attempted to elucidate different removal rates
356 and behaviors of particles in the unit processes of CSF by applying particle counting methods.

357

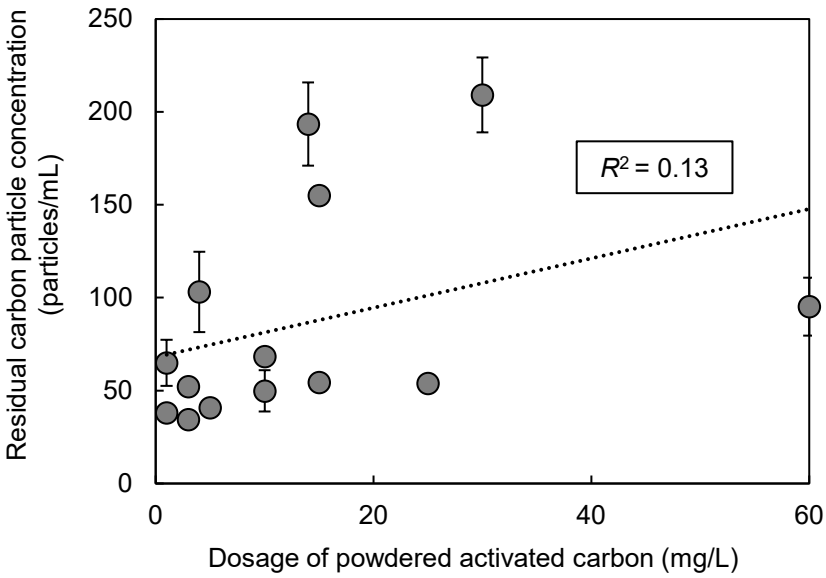

358

359 **Fig. 1.** Residual carbon particle concentration in sand filtrate vs. the dosage of powdered
360 activated carbon. The sample waters were obtained from the 14 full-scale water purification
361 plants employing the CSF process when powdered activated carbon was being injected for
362 adsorption. The dotted line indicates the regression line. Error bars indicate standard deviations

363 of three measurements, but some of them are hidden behind the symbols.

364

365

366 *3.2. Comparison of AC and clay particles during the CSF process*

367

368 After finding that the removal rate of AC particles was very different from that of turbidities
369 in full-scale plants, we conducted bench-scale CSF experiments with water containing either
370 kaolin or montmorillonite and either PAC or SPAC, to compare the fates and efficiencies of
371 removal of AC and clay particles (Fig. 2 and Fig. 3). Initial concentrations of kaolin,
372 montmorillonite, and PAC were set at 10 mg/L, and the initial concentration of SPAC was set
373 at 2 mg/L. These concentrations corresponded to 1.2×10^6, 2.3×10^4, 4.0×10^6, and 4.0×10^6
374 particles/mL, respectively. The reason for the low concentration of SPAC was the low
375 concentration required for its adsorption and the low removability of SPAC itself (Bonvin *et al.*
376 2016, Nakazawa et al. 2018).

377 PAC particles were removed largely by coagulation-flocculation and sedimentation (CS).
378 The concentration of PAC particles in the sedimentation supernatant was 2.2 logs lower than
379 the initial PAC concentration (Fig. 2). The fact that the concentration of stray, un-flocculated
380 PAC particles in the supernatant, which was determined after centrifuging the supernatant, was
381 1.8 logs lower than the total PAC in the supernatant indicated that most of particles in the
382 supernatant were coagulated to some extent, though the degree of coagulation was low. Such
383 PAC particles in the supernatant were therefore adequately removed via rapid sand filtration.
384 The total removal rate of PAC by CSF was 4.7 logs, which was within the range observed for
385 the full-scale water treatment plants (Section 3.1); therefore, the conditions under which our
386 laboratory bench-scale experiments were carried out were realistic. The overall removal rate by

387 CSF was therefore similar for SPAC and PAC, but removal of SPAC versus PAC was slightly
388 higher via CS and slightly lower via rapid sand filtration (Fig. 2).

389 Most kaolin particles were removed by CS (Fig. 2). The fact that kaolin particles in the
390 sedimentation supernatant were not as efficiently removed by centrifugation as PAC and SPAC
391 particles, however, indicated that the proportion of stray, un-flocculated kaolin particles among
392 the kaolin particles in the sedimentation supernatant was high. The removal rate via rapid sand
393 filtration of kaolin particles versus PAC and SPAC particles in the sedimentation supernatant
394 was not high because the stray, un-flocculated kaolin particles in the supernatant were not likely
395 to be removed efficiently (Nakazawa et al. 2021). The total removal rate of kaolin particles by
396 CSF was consequently 2.8 logs, which was much lower than those of PAC and SPAC (4.6±
397 0.2 logs; from comparison of numbers [CNs] 1, 2, and 3 in Table 2). The total removal rate of
398 montmorillonite clay particles by CSF in the presence of SPAC was 2.9 logs, which was also
399 lower than that of the SPAC in the same water (4.5 logs) (Fig. 3). The total removal rate of
400 montmorillonite was higher than that of kaolin because of its higher removal rate via rapid sand
401 filtration. The removal rates by CS were consequently about the same for PAC, SPAC, kaolin,
402 and montmorillonite, but the removal rates by rapid sand filtration were higher for PAC and
403 SPAC than for montmorillonite, and the removal by rapid sand filtration was the lowest for
404 kaolin. This trend was consistently observed in the 17 experimental runs that were conducted
405 in duplicate with water containing either PAC or SPAC, either kaolin or montmorillonite, one
406 kind of MP, and viruses (Fig. S6 and Table 2, where the removal rates are summarized).

407 The removal efficiency of suspended particles has conventionally been evaluated based on
408 turbidity. Because turbidity is proportional to the surface-area concentration of a given material
409 (Kissa 1999, Nakazawa et al. 2018), we calculated turbidity-equivalent removal rates based on
410 surface-area concentrations. The results were consistent with the trend of lower removal of

411 kaolin and montmorillonite (3.2 ± 0.3 logs) versus PAC and SPAC (5.0 ± 0.1 logs) when
412 concentrations were evaluated in terms of turbidity equivalents (Figs. S7 and S8 of SI).
413 The size and ZP of particles are widely recognized to be related to their removal by
414 coagulation. We also measured particle sizes and ZPs (Table 1). The particle sizes of PAC and
415 SPAC are different, but their removal by CSF followed almost similar trends. The particle sizes
416 of PAC and montmorillonite were similar (Fig. S2 and Table 1), but the trends of their removal
417 via CSF differed. The sizes of the residual particles of PAC, SPAC, and kaolin after CSF
418 treatment all fell in the range 0.2−5 μm, though the associated particle size distributions differed
419 (Fig. S9). Therefore, differences of particle sizes are unlikely to account for the lower removal
420 rates of kaolin and montmorillonite versus PAC and SPAC particles. The ZPs were all in the
421 range of −18 to −24 mV, and the ZP of kaolin, which was removed with the lowest efficiency,
422 was in the middle in this range. The ZP results therefore did not explain the lower removal rates
423 of kaolin and montmorillonite versus PAC and SPAC (Table 2 and Fig. S10). The smaller sizes
424 of particles of PAC, SPAC, kaolin, and montmorillonite after versus before CSF treatment
425 indicated the preferential removal of large particles (Fig. S9). This preferential removal of large
426 particles was consistent with our previous observations of PAC and SPAC removal (Nakazawa
427 et al. 2021, Nakazawa et al. 2018).
428 The results in Section 3.1 showed that the concentrations of AC particles in sand filtrate
429 were very low compared to the turbidities of the same water, and turbidity removal was not
430 correlated with AC removal. These patterns were caused by the low removal rates of clay
431 particles by rapid sand filtration (2.8 ± 0.2 logs; from CNs 4, 5, and 6 in Table 2) versus AC
432 particles (4.6 ± 0.2 logs; from CNs 1, 2, and 3 in Table 2). Fig. 4 shows the calculated ratios of
433 clay particles to AC particles in raw water before treatment, sedimentation supernatant, and
434 sand filtrate in terms of turbidity equivalents (surface area concentrations). In raw water and

435 sedimentation supernatant, clay particles and AC particles were present in similar ratios, but in
436 sand filtrate, the very high ratio of clay particles to AC particles indicated that clay particles
437 accounted for the turbidity of the sand filtrate.

438 In the practice of water treatment, AC are added with great care to ensure that there is no
439 leakage. However, this study showed that AC particles were two orders of magnitude more
440 removable than clay particles; most of the particles remaining after filtration were probably clay
441 particles, and only a small portion (on the order of 1%) could have been AC particles (Fig. 4).
442 The apparent problem of leakage of AC particles is not their leakage rate but rather the fact that
443 AC particles are black and conspicuous. As a result of the Cryptosporidium problem (Medema
444 *et al.* 2009), the turbidity of water after CSF treatment is now strictly controlled, and the number
445 of particles is monitored besides the turbidity. The concentration of particles after CSF
446 treatment has been reported to be 1000 to 10,000 particles/mL (Watanabe and Ogino 2006).
447 One percent of these concentrations (i.e., 10–100 particles/mL) is the same order of magnitude
448 as the measured concentrations of AC particles (Section 3.1). If the particle concentration is
449 maintained at less than 10,000 particles/mL, the concentration of residual AC particles when
450 AC is injected will be less than 100 particles/mL, a level that will not cause any problem
451 associated with leakage of carbon particles based on the plant data reported in Section 3.1.
452
453
454

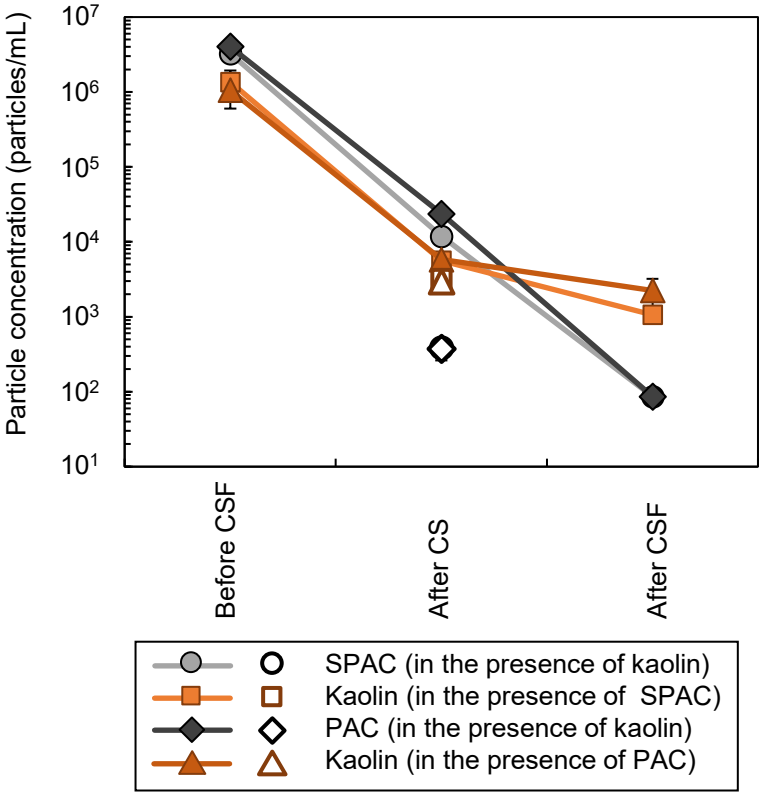

Fig. 2. Behaviors of PAC, SPAC, and kaolin during the CSF process. Kaolin and either PAC or SPAC were added simultaneously. The open symbols indicate the data measured after centrifugation. Data from Run 1 and Run 2. Details of the experimental condition are presented in Table S2. Error bars indicate standard deviations of measurements, but some of them are hidden behind the symbols.

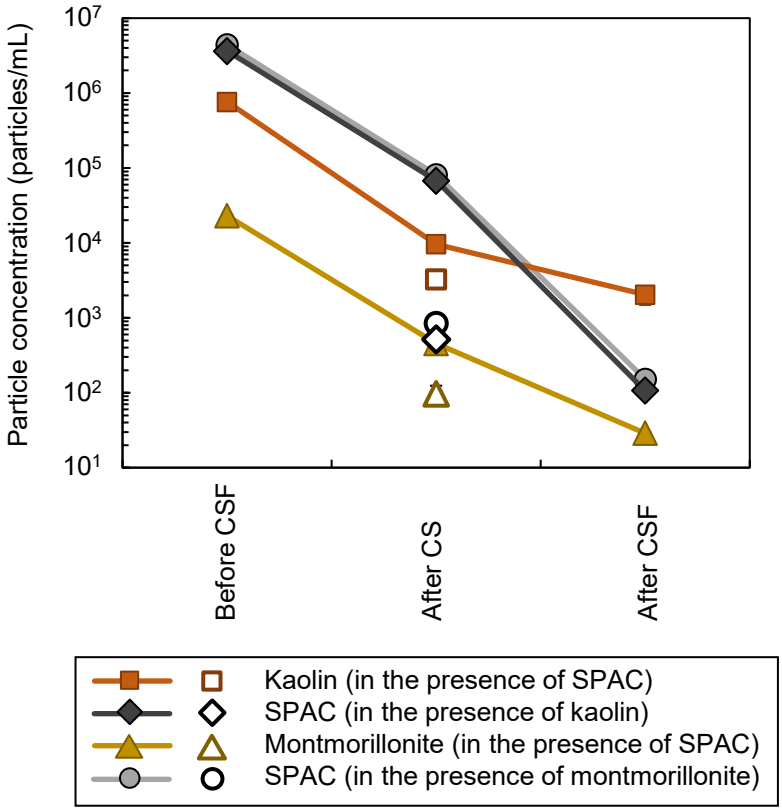

Fig. 3. Behaviors of kaolin, montmorillonite, and SPAC during the CSF process. Either kaolin or montmorillonite and SPAC were added simultaneously. The open symbols indicate the data measured after centrifugation. Data from Runs 3, 4, 5, and 6. Details of the experimental conditions are presented in Table S2. Error bars indicate standard deviations of experiments, but some of them are hidden behind the symbols.

Table 2

Removal rates of particles and experimental conditions.

Comparison number (CN)	Number of experimental runs	Target particle	Average Log-removal rate ± Log-SD of target particle by CS	Average Log-removal rate ± Log-SD of target particle by CSF			Initial concentration of target particle		Major coexisting substance with concentration > 1 mg/L	Coagulant dose	Run No.
							mg/L	particles/mL or copies/mL		mg-Al/L	
1	4	PAC	2.2±0.1	4.7±0.1		4.6±0.2	10	4.0×10^{6}	Kaolin 10 mg/L	3	2, 8, 11, and 12
2	7	SPAC	2.1±0.3	4.7±0.2	4.6±0.2		2	4.9×10^{6}	Kaolin 10 mg/L	3	1, 3, 4, 7, 9, 10, and 13
3	2	SPAC	1.7±0.1	4.5±0.0			2	4.4×10^{6}	Montmorillonite 10 mg/L	3	5 and 6
4	4	kaolin	2.1±0.1	2.7±0.0	2.8±0.2	2.8±0.2	10	8.1×10^{5}	PAC 10 mg/L	3	2, 8, 11, and 12
5	7	kaolin	2.2±0.2	2.8±0.2			10	9.5×10^{5}	SPAC 2 mg/L	3	1, 3, 4, 7, 9, 10, and 13
6	2	Montmor-illonite	1.7±0.0	2.9±0.0			10	2.3×10^{4}	SPAC 2 mg/L	3	5 and 6
7	1	PA	ND	2.9	2.9±0.2	2.9±0.3	0.001	6	PAC 10 mg/L, Kaolin 10 mg/L	3	8
8	3	PA	1.4±0.1	2.7±0.2			0.001	7	SPAC 2mg/L, Kaolin 10 mg/L	3	3, 4, and 7
9	2	PA	2.0±0.0	3.1±0.0			0.001	17	SPAC 2mg/L, Montmorillonite 10 mg/L	3	5 and 6
10	2	PE	2.4±0.1	3.2±0.0	3.2±0.1		0.001	11	PAC 10 mg/L, Kaolin 10 mg/L	3	11 and 12
11	1	PE	2.5	3.3			0.001	10	SPAC 2mg/L, Kaolin 10 mg/L	3	13
12	1	PSi	ND	2.6	2.6±0.1		0.001	5	PAC 10 mg/L, Kaolin 10 mg/L	3	1
13	1	PSi	ND	2.5			0.001	5	SPAC 2mg/L, Kaolin 10 mg/L	3	2
14	2	PMMoV	3.3±0.1	3.6±0.1		3.5±0.3	Not applicable	10^{7}–10^{8}	PAC 10 mg/L, Kaolin 10 mg/L	3	11 and 12
15	2	MS2	2.6±0.3	3.4±0.4			Not applicable	10^{7}–10^{8}	PAC 10 mg/L, Kaolin 10 mg/L	3	11 and 12
16	2	PA	1.7±0.1	2.6±0.0			0.001	14	SPAC 2 mg/L	1.5	14 and 15
17	2	PA-pw	1.7±0.1	2.2±0.2			0.001	16	SPAC 2 mg/L, Kaolin 10 mg/L	3	9 and 10
18	2	PA-md	1.1±0.0	2.6±0.1			0.001	12	SPAC 2 mg/L	1.5	16 and 17

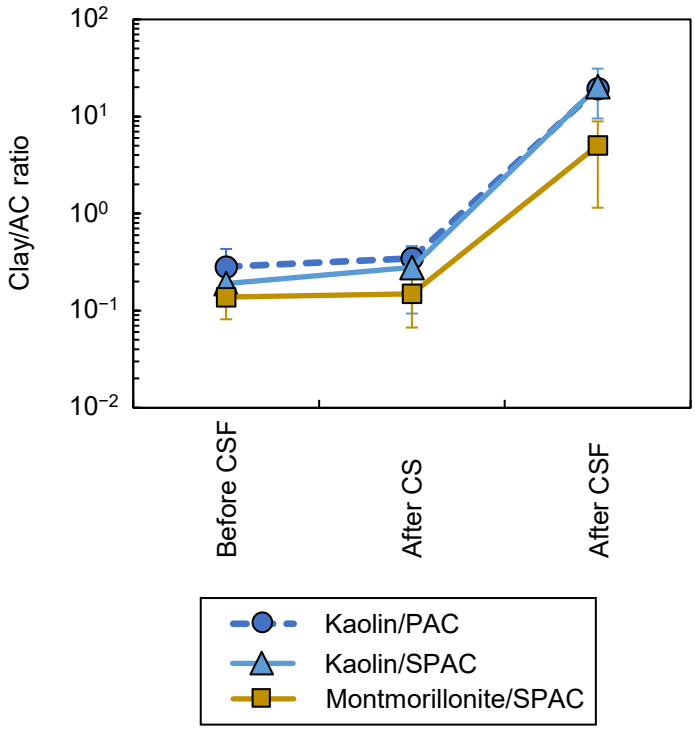

Fig. 4. Ratio of clay particles to activated carbon particles quantified by surface-area concentrations. Either kaolin or montmorillonite and either PAC or SPAC were added simultaneously. Data from Runs 1, 2, 3, 4, 5, 6, 7, 8, 9 10, 11, 12 and 13. Details of the experimental condition are presented in Table S2. Error bars indicate standard deviations of experiments, but some of them are hidden behind the symbols.

3.3. Comparing MP versus clay/AC particles during the CSF process

This section focuses on the concentrations of MPs. Total removal rates of PE, PA, and PSi by CSF were almost the same—2.9±0.3 logs (from CNs 7, 8, 9, 10, 11, 12, and 13 in Table 2)—a rate that was much lower than those of SPAC and PAC particles but similar to that of kaolin particles (Fig. 5 and Fig. S11). PA removal was lower than PE removal by CS, but PA removal by rapid sand filtration was higher. As a result, the total removals of PA and PE by CSF were similar. These trends were almost unchanged by conversion to turbidity equivalents

using surface-area concentrations (Fig. S12). Zhou et al. (2021) have reported that MPs with relatively high densities are removed more efficiently by CS. However, we did not observe such a trend: in our experiments, PE particles, which have a lower density than PA particles, were removed with higher efficiency than the latter. Zhou et al. (2021) used waters containing only extremely high concentration of MPs (100–1000 mg/L). Floc particles should therefore have been formed mainly by MPs, and the density of the floc particles would have been largely determined by the density of the MPs. In contrast, we mimicked a normal water treatment situation wherein MPs were present in trace amounts compared to clay and ACs. Under these conditions, the density of floc particles was determined by clay and AC particles rather than by MP particles. The density of the MPs would consequently not have influenced their removal by CS. We feel that the less negative ZP of PA compared to PE was related to its higher removal by CS because the same trend was observed before/after PA weathering (detailed in Section 3.5). It should be noted, however, that ZP could not explain the differences in removal rates between very different types of particles (clay versus AC, see section 3.2).

The observed removal rate of PE, PA, and PSi by CSF, 2.9±0.3 logs, exceeded rates reported previously (~1 log) (Pivokonsky et al. 2018, Wang et al. 2020b, Zhang et al. 2020), but direct quantitative comparisons between our data and previous data are inappropriate because particle removal rates by CSF are highly dependent on the design of the CSF and operating conditions such as coagulant dose and filtration speed. This study showed that a rate of removal of MPs as high as ~3 logs (99.9%) can be achieved. More importantly, the fact that the removal rate of MP particles was comparable to that of clay particles (kaolin and montmorillonite) means that if satisfactory removal of turbidity—the principal metric of the adequacy of drinking water purification—is consistently achieved, a similar level of removal can be expected for MP particles. In other words, MP particles are not unusually difficult to

remove. Of course, the removability of particles depends on the properties of the particles, but this trend of removal was also observed for MPs after weathering, as described in Section 3.5.

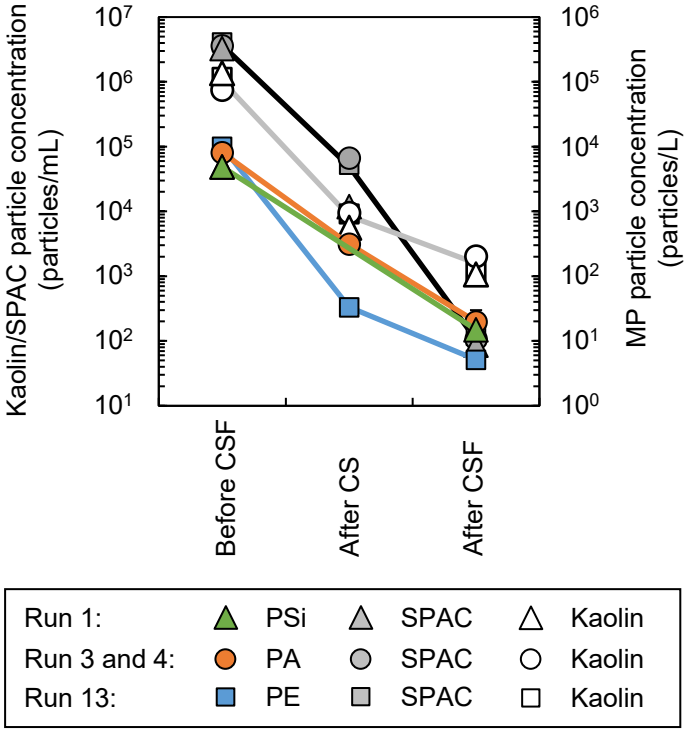

Fig. 5. Behavior of PE, PA, and PSi during the CSF process. PA, Psi, and PE were each treated by CSF in the presence of SPAC and kaolin. Data from Runs 1, 3, 4, and 13. Details of the experimental condition are presented in Table S2. Error bars indicate standard deviations of experiments, but some of them are hidden behind the symbols.

3.4. Comparison of viruses versus clay/AC particles during CSF processes

Overall removal rates of viruses by CSF were 3.6 logs for the PMMoV strain and 3.4 logs for the MS2 strain (Fig. 6). These rates were higher than those for kaolin and montmorillonite particles but lower than those for PAC and SPAC particles (Fig. 6 and Table 2). The fact that the abundances of both PMMoV and MS2 decreased greatly after CS (3.3 logs and 2.6 logs,

532 respectively) compared with the other types of particles (clay, AC, and MPs) resulted in high
533 total removals of viruses by CSF, though the removal by rapid sand filtration was not high (<0.8
534 log) (Fig. 6).

535 The relationship between the size of particles and their removal by a sand filter has been
536 studied theoretically, and it is commonly understood that the removal rate of particles around 1
537 μm in size is the lowest. The removal of smaller particles as well as larger particles is higher
538 because of Brownian transport (Edzwald 2011). The particle sizes of the MS2 and PMMoV
539 strains are diameter 26 nm (spherical particle) and diameter 18× length 300 nm (rod-shaped
540 particle), respectively, and according to this filtration theory, these viruses should have been
541 removed with higher efficiency than SPAC, which has a particle diameter of ~1 μm (Figs. S2
542 and S9). However, the removal rate of viruses by rapid sand filtration was clearly lower than
543 that of SPAC (Figs. 2 and 6). We feel that most of the viruses remaining after CS were single-
544 strand, un-flocculated particles with insufficient charge neutralization and consequently a small
545 probability of attachment onto sand grains, as described in Section 3.2 in the case of kaolin
546 particles.

547 The observed virus removal rates (3.5±0.3 logs; from CN 14 and 15 in Table 2) were high
548 compared to those previously reported (Asami et al. 2016, Kato et al. 2018, Shirasaki et al.
549 2018) and could be related to the CSF operating conditions. For example, it is very reasonable
550 that CS removal of particulate matter, including virus particles, would be highly dependent on
551 coagulant dosage (Shirasaki *et al.* 2009, Zhou et al. 2021). Shirasaki et al. (2018) have reported
552 1.5−2.0 log removal of the PMMoV and MS2 strains by CSF, but their filter depth was only 20
553 cm, and their filtration velocity was 120 m d^{-1}, which was higher than ours (90 m d^{-1}). The
554 coagulant dosages in the CSF experiments of Kato et al. (2018) were 0.8–2 mg/L and therefore
555 lower than our dosage of 3 mg/L, though the DOC of their raw water was higher than that of
556 ours. Asami et al. (2016) have reported a PMMoV removal of 2.4 logs by a full-scale water

purification plant employing CSF. The fact that the turbidity of treated waters in that plant after CSF was not low, 1−3 formazin attenuation units, suggests that clay particle removal by the plant was not as high as the removal by our CSF plant. Nonetheless, our data were in accordance with the previous data in two respects. First, the removal of PMMoV was somewhat higher than removal of turbidity. In the study of Asami et al. (2016), PMMoV removal was 2.4 logs, and turbidity removal was 1.5–2 logs. In our data, PMMoV removal was 3.6 logs (Fig. 6), and the turbidity-equivalent removal of kaolin particles was 3.4 logs (Fig. S8). Second, the virus removal by CSF was accomplished largely by CS, and the contribution of rapid sand filtration was marginal (Kato et al. 2018). We also feel that the presence of AC may have accelerated the removal of viruses by coagulation in an synergetic way because AC can to some extent adsorb and remove viruses (Matsushita *et al.* 2013). In our data, however, the viruses were not removed by PAC alone (Fig. 6).

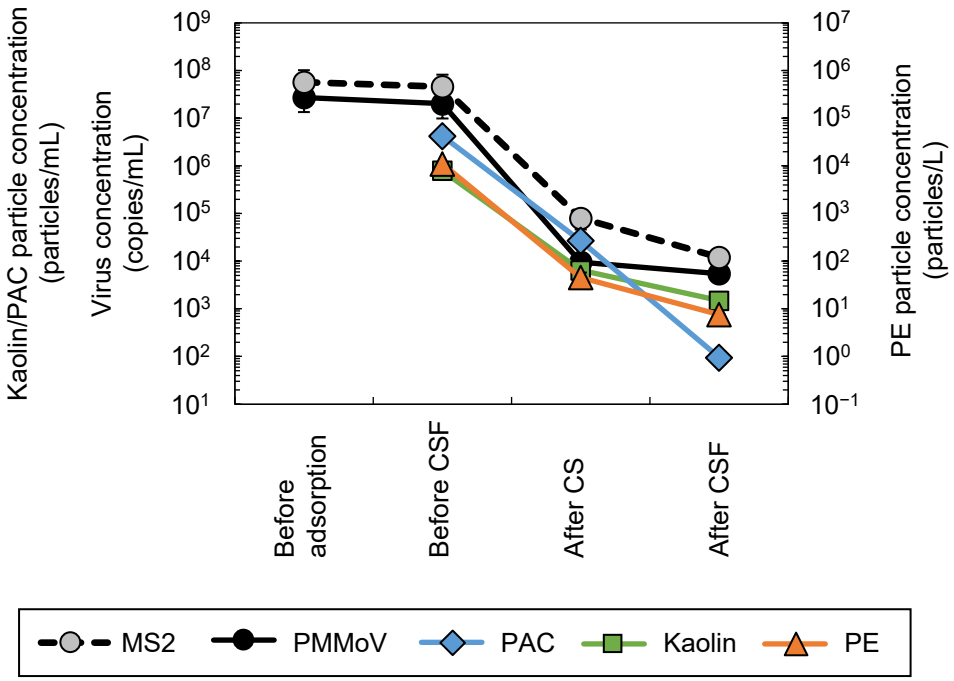

572 **Fig. 6.** Behavior of PMMoV and MS2 during the CSF process. Vertical axis on left side is for
573 PMMoV, MS2, Kaolin, and PAC concentrations, whereas vertical axis on right side is for PE
574 concentration. PMMoV, MS2, kaolin, PAC, and PE were added simultaneously. Data from
575 Runs 11 and 12. Details of the experimental condition are presented in Table S2. Error bars
576 indicate standard deviations of experiments, but some of them are hidden behind the symbols.
577
578
579
580 *3.5. Effects of weathering on MP removal*
581
582 It has been reported that MPs can be mechanically/photochemically weathered after being
583 released to the environment (Sun et al. 2020), but the effect of weathering on the rate of their
584 removal by CSF has been unclear. We began the experiments with photochemical weathering
585 and examined the effects of the weathering by comparing weathered PA particles that had been
586 exposed to the sun for 68 days (PA-pw) with virgin ones. The removal rate of the PA-pw by CS
587 was 1.7 logs, which was slightly higher than that of the virgin PA (1.4 logs) (Fig. 7). However,
588 its removal rate by rapid sand filtration was slightly lower (0.5 log) than that of virgin PA (1.3
589 logs). The result was a higher residual concentration of PA-pw particles than virgin PA particles
590 in sand filtrate. Prior to carrying out these experiments, we thought that the hydrophilicity of
591 PA might be changed by exposure to the ultraviolet (UV) radiation in sunlight, as reported for
592 the UV in artificial light (Lin et al. 2020). With this mind, we compared the physical properties
593 of PA and PA-pw. However, there was no difference in the FTIR spectrum before and after
594 exposure to sunlight (Fig. S13). Exposure of the PA to sunlight for 68 days may not have been
595 sufficient to cause a change of the FTIR spectrum. Lin et al. (2020) used UV and vacuum
596 ultraviolet (VUV) lamps and irradiated polyvinylchloride and polystyrene MPs at 1.8 (UV) or
597 36 (VUV) kJ/m^2. In contrast, we estimated the UV irradiation intensity associated with the 68

days of our experiment to be 0.21 kJ/m^2 based on the global horizontal intensity of irradiance and glass transmittance. This intensity was merely ~10% of the intensity used by Lin et al. (2020). Particle shape (Fig. 8) and size (Fig. S2 and Table 1) were not changed by the 68-day exposure, but the ZP decreased somewhat after sunlight exposure (Fig. S14). Although it seems unlikely that this change of ZP would have caused a great change in the particle removal rate, it is possible that reducing the magnitude of the negative charge caused a small increase in the removal rate of the PA particles via CS and a small decrease via sand filtration. This interpretation is consistent with the result described in Section 3.3 that the removal rates of the PE particles, which had a less negative ZP than the PA particles, were higher via CS but lower via rapid sand filtration than the removal rates of the PA particles (Table 2).

We also examined the effect of mechanical damage on PA removal by placing the PA in a ball-milling. The size of the PA particles was not changed much (Fig. S2 and Table 1). Instead, the particles were abraded or deformed rather than crushed by the ball milling (Fig. 8). The FTIR spectrum was not changed (Fig. S13), but the observed ZP became slightly more negative (Fig. S14). The fate of PA during the CSF process was clearly changed by the mechanical damage (Fig. 7). The removal rate by CS was decreased from 1.7 logs (PA) to 1.1 logs (PA-md). However, the removal rate by rapid sand filtration increased from 0.9 log (virgin PA) to 1.5 logs. The overall removal of PA by CSF was unchanged by mechanical damage. This effect of mechanical weathering on the removal rate and ZP of PA was opposite to the effect of photochemical weathering. The negative shift of the ZP of PA caused by mechanical weathering might enhance its removability via rapid sand filtration.

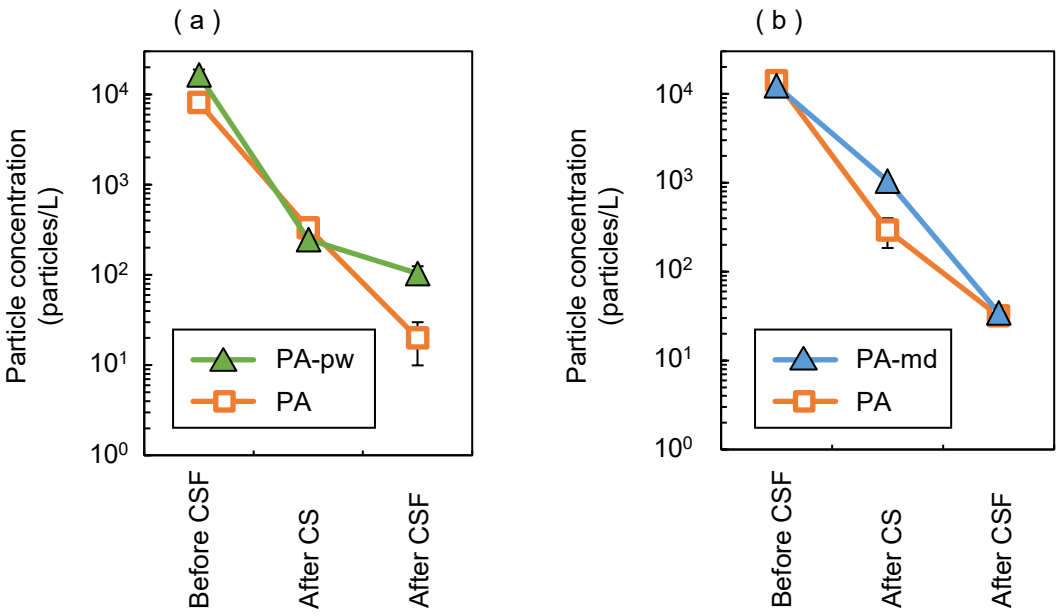

Fig. 7. Effect of photochemical/mechanical weathering on the removal of MP particles during CSF process. Panel a: PA and PA-pw were each added in the presence of kaolin and SPAC simultaneously (Run 3, 4, 9, and 10). Panel b: PA or PA-md was each added in the presence of SPAC simultaneously (Run 14, 15, 16, and 17). Details of the experimental conditions are presented in Table S2. Error bars indicate standard deviations of experiments, but some of them are hidden behind the symbols.

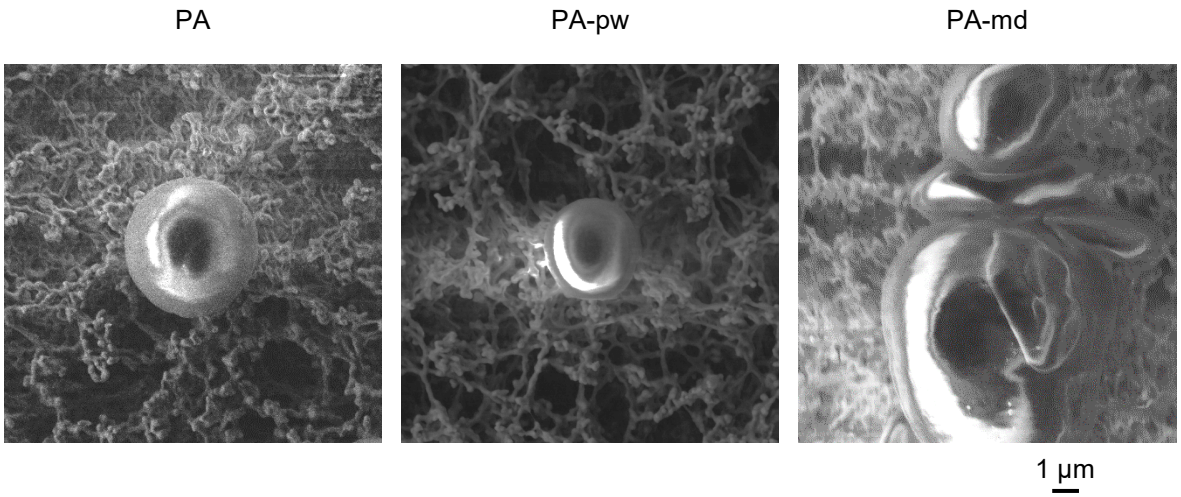

Fig. 8. Field-emission scanning electron microscope images of PA particles before and after weathering.

4. Conclusions

The results of this research led to the following conclusions:

1) The present study determined, for the first time, the residual concentrations of carbon particles remaining in sand filtrate in actual, full-scale water purification plants employing a CSF process when PAC was used for the adsorption treatment; the range of the concentrations was < 200 particles/mL. Since no customer complaints, this concentration with could be considered a rough indication for the goal of treatment with SPAC.
2) CS greatly decreased the concentrations of all target particles tested (kaolin, montmorillonite, PAC, SPAC, PA, PE, PSi, MS2, and PMMoV). Rapid sand filtration greatly decreased the concentrations of PAC and SPAC, but the decreases in the concentrations of the other particles by rapid sand filtration were not large. In particular, viruses (strains PMMoV and MS2) were greatly removed by CS, but they were removed only a little by rapid sand filtration. In the case of kaolin, the high proportion of stray, un-flocculated particles in the sedimentation supernatant led to low removal by rapid sand filtration of particles in the supernatant.
3) The particle removal rates by CSF were 4.6±0.2 logs for PAC and SPAC, 3.5±0.3 logs for PMMoV and MS2, 2.9±0.3 logs for PA, PE, and PSi MPs, and 2.8±0.2 logs for kaolin and montmorillonite. The PA, PE, and PSi (particle sizes: 4.8−6.5 μm) could be removed by CSF at a rate similar to the rate of removal of clay particles (kaolin: 5.6 μm, montmorillonite: 12 μm). The removal rates of the MPs (2.9±0.3 logs) were slightly lower than that of turbidity caused by clays (3.2±0.3 logs). The removal rate of the viruses by CSF was higher than that of clay particles. The turbidity-equivalent removal rates were 5.0±0.1 logs for PAC and SPAC and 3.2±0.3 logs for kaolin and

montmorillonite. These differences in removal rates between particles were not explained by particle size or ZP. However, for kaolin, montmorillonite, PAC, and SPAC, which have wide particle-size distributions, smaller particles of each remained after treatment.

4) The ratio of clay/AC particles became very high after CSF treatment because AC particles were removed at rates about 2 orders of magnitude higher than the rates of removal of clay particles. Consequently, clay particles contributed predominantly to the turbidity in sand filtrate, even when PAC was added to the raw water.

5) Mechanical/photochemical weathering of PA affected the removal of PA in CS and rapid sand filtration to some extent. PA-pw was removed by CS slightly higher than virgin PA. During rapid sand filtration, PA-pw was removed at a somewhat lower rate than virgin PA. The removal rate of PA-md by CS and rapid sand filtration decreased and increased, respectively, relative to the removal rates of virgin PA. The change of ZP by the mechanical/photochemical weathering may have caused these changes of PA removals by CS and rapid sand filtration. However, no clear difference was apparent in the FTIR spectra of PA, PA-pw, and PA-md.

Acknowledgments

This study was supported by a Grant-in-Aid for Scientific Research S (JP16H06362) and a Research Fellowship for Yong Scientists (JP19J11070) from the Japan Society for the Promotion of Science. The field samplings were helped by some of the members of a Health and Labour Sciences Research project (Grant number 19LA1005, the Ministry of Health, Labour and Welfare of Japan).

References

682 Adamis, Z. and Williams, R.B. (2005) Bentonite, kaolin, and selected clay minerals, World
683 Health Organization, Geneva, Switzerland.
684 Asami, T., Katayama, H., Torrey, J.R., Visvanathan, C. and Furumai, H. (2016) Evaluation of
685 virus removal efficiency of coagulation-sedimentation and rapid sand filtration processes in a
686 drinking water treatment plant in Bangkok, Thailand. Water Research 101, 84-94.
687 Bonvin, F., Jost, L., Randin, L., Bonvin, E. and Kohn, T. (2016) Super-fine powdered
688 activated carbon (SPAC) for efficient removal of micropollutants from wastewater treatment
689 plant effluent. Water Research 90, 90-99.
690 Cho, K., An, B.M., So, S., Chae, A. and Song, K.G. (2020) Simultaneous control of algal
691 micropollutants based on ball-milled powdered activated carbon in combination with
692 permanganate oxidation and coagulation. Water Research 185, 116263.
693 Dris, R., Gasperi, J., Saad, M., Mirande, C. and Tassin, B. (2016) Synthetic fibers in
694 atmospheric fallout: A source of microplastics in the environment? Marine Pollution Bulletin
695 104(1), 290-293.
696 Edzwald, J.K. (2011) Water quality & treatment A handbook on drinking water, American
697 Water Works Association, American Society of Civil Engineers, McGraw-Hill, Denver, CO
698 80235 USA.
699 Elizalde-Velázquez, G.A. and Gómez-Oliván, L.M. (2021) Microplastics in aquatic
700 environments: A review on occurrence, distribution, toxic effects, and implications for human
701 health. Science of The Total Environment 780, 146551.
702 Freeman, S., Booth, A.M., Sabbah, I., Tiller, R., Dierking, J., Klun, K., Rotter, A., Ben-David,
703 E., Javidpour, J. and Angel, D.L. (2020) Between source and sea: The role of wastewater
704 treatment in reducing marine microplastics. Journal of Environmental Management 266,
705 110642.

Iqbal, S., Xu, J., Allen, S.D., Khan, S., Nadir, S., Arif, M.S. and Yasmeen, T. (2020) Unraveling consequences of soil micro- and nano-plastic pollution on soil-plant system: Implications for nitrogen (N) cycling and soil microbial activity. Chemosphere 260, 127578.

Iwasaki, S., Isobe, A., Kako, S.i., Uchida, K. and Tokai, T. (2017) Fate of microplastics and mesoplastics carried by surface currents and wind waves: A numerical model approach in the Sea of Japan. Marine Pollution Bulletin 121(1), 85-96.

Kato, R., Asami, T., Utagawa, E., Furumai, H. and Katayama, H. (2018) Pepper mild mottle virus as a process indicator at drinking water treatment plants employing coagulation-sedimentation, rapid sand filtration, ozonation, and biological activated carbon treatments in Japan. Water Res 132, 61-70.

Kissa, E. (1999) Dispersions characterization, testing, and measurement, Taylor & Francis, New York.

Koelmans, A.A., Mohamed Nor, N.H., Hermsen, E., Kooi, M., Mintenig, S.M. and De France, J. (2019) Microplastics in freshwaters and drinking water: Critical review and assessment of data quality. Water Research 155, 410-422.

Kögel, T., Bjorøy, Ø., Toto, B., Bienfait, A.M. and Sanden, M. (2020) Micro- and nanoplastic toxicity on aquatic life: Determining factors. Science of The Total Environment 709, 136050.

Kosuth, M., Mason, S.A. and Wattenberg, E.V. (2018) Anthropogenic contamination of tap water, beer, and sea salt. Plos One 13(4), e0194970.

Lin, J., Yan, D., Fu, J., Chen, Y. and Ou, H. (2020) Ultraviolet-C and vacuum ultraviolet inducing surface degradation of microplastics. Water Research 186, 116360.

Ma, B., Xue, W., Hu, C., Liu, H., Qu, J. and Li, L. (2019) Characteristics of microplastic removal via coagulation and ultrafiltration during drinking water treatment. Chemical Engineering Journal 359, 159-167.

730 Matsushita, T., Suzuki, H., Shirasaki, N., Matsui, Y. and Ohno, K. (2013) Adsorptive virus
731 removal with super-powdered activated carbon. Separation and Purification Technology 107,
732 79-84.
733 Medema, G., Teunis, P., Blokker, M., Deere, D., Davison, A., Charles, P. and Loret, J.-F.
734 (2009) Risk assessment of Cryptosporidium in drinking water, World Health Organization,
735 Geneva, Switzerland.
736 Mintenig, S.M., Löder, M.G.J., Primpke, S. and Gerdts, G. (2019) Low numbers of
737 microplastics detected in drinking water from ground water sources. Science of The Total
738 Environment 648, 631-635.
739 Naik, R.A., Rowles, L.S., Hossain, A.I., Yen, M., Aldossary, R.M., Apul, O.G., Conkle, J.
740 and Saleh, N.B. (2020) Microplastic particle versus fiber generation during photo-
741 transformation in simulated seawater. Science of The Total Environment 736, 139690.
742 Nakazawa, Y., Abe, T., Matsui, Y., Shirasaki, N. and Matsushita, T. (2021) Stray particles as
743 the source of residuals in sand filtrate: Behavior of superfine powdered activated carbon
744 particles in water treatment processes. Water Research 190, 116786.
745 Nakazawa, Y., Matsui, Y., Hanamura, Y., Shinno, K., Shirasaki, N. and Matsushita, T. (2018)
746 Identifying, counting, and characterizing superfine activated-carbon particles remaining after
747 coagulation, sedimentation, and sand filtration. Water Research 138, 160-168.
748 Ninomiya, Y., Kimura, K., Sato, T., Kakuda, T., Kaneda, M., Hafuka, A. and Tsuchiya, T.
749 (2020) High-flux operation of MBRs with ceramic flat-sheet membranes made possible by
750 intensive membrane cleaning: Tests with real domestic wastewater under low-temperature
751 conditions. Water Research 181, 115881.
752 Pan, L., Takagi, Y., Matsui, Y., Matsushita, T. and Shirasaki, N. (2017) Micro-milling of
753 spent granular activated carbon for its possible reuse as an adsorbent: Remaining capacity and
754 characteristics. Water Research 114, 50-58.

Pivokonsky, M., Cermakova, L., Novotna, K., Peer, P., Cajthaml, T. and Janda, V. (2018) Occurrence of microplastics in raw and treated drinking water. Science of The Total Environment 643, 1644-1651.

Rajala, K., Grönfors, O., Hesampour, M. and Mikola, A. (2020) Removal of microplastics from secondary wastewater treatment plant effluent by coagulation/flocculation with iron, aluminum and polyamine-based chemicals. Water Research 183, 116045.

Revel, M., Châtel, A. and Mouneyrac, C. (2018) Micro(nano)plastics: A threat to human health? Current Opinion in Environmental Science & Health 1, 17-23.

Rodrigues, M.O., Abrantes, N., Gonçalves, F.J.M., Nogueira, H., Marques, J.C. and Gonçalves, A.M.M. (2018) Spatial and temporal distribution of microplastics in water and sediments of a freshwater system (Antuã River, Portugal). Science of The Total Environment 633, 1549-1559.

Shen, M., Song, B., Zhu, Y., Zeng, G., Zhang, Y., Yang, Y., Wen, X., Chen, M. and Yi, H. (2020) Removal of microplastics via drinking water treatment: Current knowledge and future directions. Chemosphere 251, 126612.

Shirasaki, N., Matsushita, T., Matsui, Y., Marubayashi, T. and Murai, K. (2016) Investigation of enteric adenovirus and poliovirus removal by coagulation processes and suitability of bacteriophages MS2 and φX174 as surrogates for those viruses. Science of The Total Environment 563-564, 29-39.

Shirasaki, N., Matsushita, T., Matsui, Y. and Murai, K. (2017) Assessment of the efficacy of membrane filtration processes to remove human enteric viruses and the suitability of bacteriophages and a plant virus as surrogates for those viruses. Water Research 115, 29-39.

Shirasaki, N., Matsushita, T., Matsui, Y., Urasaki, T. and Ohno, K. (2009) Comparison of behaviors of two surrogates for pathogenic waterborne viruses, bacteriophages Qβ and MS2, during the aluminum coagulation process. Water Research 43(3), 605-612.

780 Shirasaki, N., Matsushita, T., Matsui, Y. and Yamashita, R. (2018) Evaluation of the
781 suitability of a plant virus, pepper mild mottle virus, as a surrogate of human enteric viruses
782 for assessment of the efficacy of coagulation–rapid sand filtration to remove those viruses.
783 Water Research 129, 460-469.
784 Skaf, D.W., Punzi, V.L., Rolle, J.T. and Kleinberg, K.A. (2020) Removal of micron-sized
785 microplastic particles from simulated drinking water via alum coagulation. Chemical
786 Engineering Journal 386, 123807.
787 Sun, Y., Yuan, J., Zhou, T., Zhao, Y., Yu, F. and Ma, J. (2020) Laboratory simulation of
788 microplastics weathering and its adsorption behaviors in an aqueous environment: A
789 systematic review. Environmental Pollution 265, 114864.
790 Syberg, K., Khan, F.R., Selck, H., Palmqvist, A., Banta, G.T., Daley, J., Sano, L. and
791 Duhaime, M.B. (2015) Microplastics: addressing ecological risk through lessons learned.
792 Environmental Toxicology and Chemistry 34(5), 945-953.
793 Uurasjärvi, E., Hartikainen, S., Setälä, O., Lehtiniemi, M. and Koistinen, A. (2020)
794 Microplastic concentrations, size distribution, and polymer types in the surface waters of a
795 northern European lake. Water Environment Research 92(1), 149-156.
796 Wang, C., Xian, Z., Jin, X., Liang, S., Chen, Z., Pan, B., Wu, B., Ok, Y.S. and Gu, C. (2020a)
797 Photo-aging of polyvinyl chloride microplastic in the presence of natural organic acids. Water
798 Research 183, 116082.
799 Wang, Y., Wang, X., Li, Y., Li, J., Liu, Y., Xia, S. and Zhao, J. (2021) Effects of exposure of
800 polyethylene microplastics to air, water and soil on their adsorption behaviors for copper and
801 tetracycline. Chemical Engineering Journal 404, 126412.
802 Wang, Z., Lin, T. and Chen, W. (2020b) Occurrence and removal of microplastics in an
803 advanced drinking water treatment plant (ADWTP). Science of The Total Environment 700,
804 134520.

Wang, Z., Sedighi, M. and Lea-Langton, A. (2020c) Filtration of microplastic spheres by biochar: removal efficiency and immobilisation mechanisms. Water Research 184, 116165.

Watanabe, H. and Ogino, Y. (2006) Investigation of water by a particle counter (in Japanese). ENVIRONMENTAL CONSERVATION ENGINEERING 35(2), 147-151.

WHO (2019) Microplastics in drinking-water, World Health Organization, Geneva, Switzerland.

Wong, J.K.H., Lee, K.K., Tang, K.H.D. and Yap, P.-S. (2020) Microplastics in the freshwater and terrestrial environments: Prevalence, fates, impacts and sustainable solutions. Science of The Total Environment 719, 137512.

Wu, P., Huang, J., Zheng, Y., Yang, Y., Zhang, Y., He, F., Chen, H., Quan, G., Yan, J., Li, T. and Gao, B. (2019) Environmental occurrences, fate, and impacts of microplastics. Ecotoxicology and Environmental Safety 184, 109612.

Zhang, Y., Diehl, A., Lewandowski, A., Gopalakrishnan, K. and Baker, T. (2020) Removal efficiency of micro- and nanoplastics (180 nm–125 μm) during drinking water treatment. Science of The Total Environment 720, 137383.

Zhou, G., Wang, Q., Li, J., Li, Q., Xu, H., Ye, Q., Wang, Y., Shu, S. and Zhang, J. (2021) Removal of polystyrene and polyethylene microplastics using PAC and $FeCl_3$ coagulation: Performance and mechanism. Science of The Total Environment 752, 141837.

Zhou, Y., Wang, J., Zou, M., Jia, Z., Zhou, S. and Li, Y. (2020) Microplastics in soils: A review of methods, occurrence, fate, transport, ecological and environmental risks. Science of The Total Environment 748, 141368.

Zhu, K., Jia, H., Sun, Y., Dai, Y., Zhang, C., Guo, X., Wang, T. and Zhu, L. (2020a) Long-term phototransformation of microplastics under simulated sunlight irradiation in aquatic environments: Roles of reactive oxygen species. Water Research 173, 115564.

Zhu, L., Zhao, S., Bittar, T.B., Stubbins, A. and Li, D. (2020b) Photochemical dissolution of buoyant microplastics to dissolved organic carbon: Rates and microbial impacts. Journal of Hazardous Materials 383, 121065.

Highlights

- Activated carbon in water treatment plant sand filtrate was 40−200 particles/mL
- The order of removal rates were activated carbon >> viruses >> clay ≈ microplastics
- Coagulation-sedimentation accounted for most virus, clay, and microplastic removal
- These particles were removed by rapid sand filtration less than by activated carbon
- Weathering changed the zeta potential and removal of microplastics a little

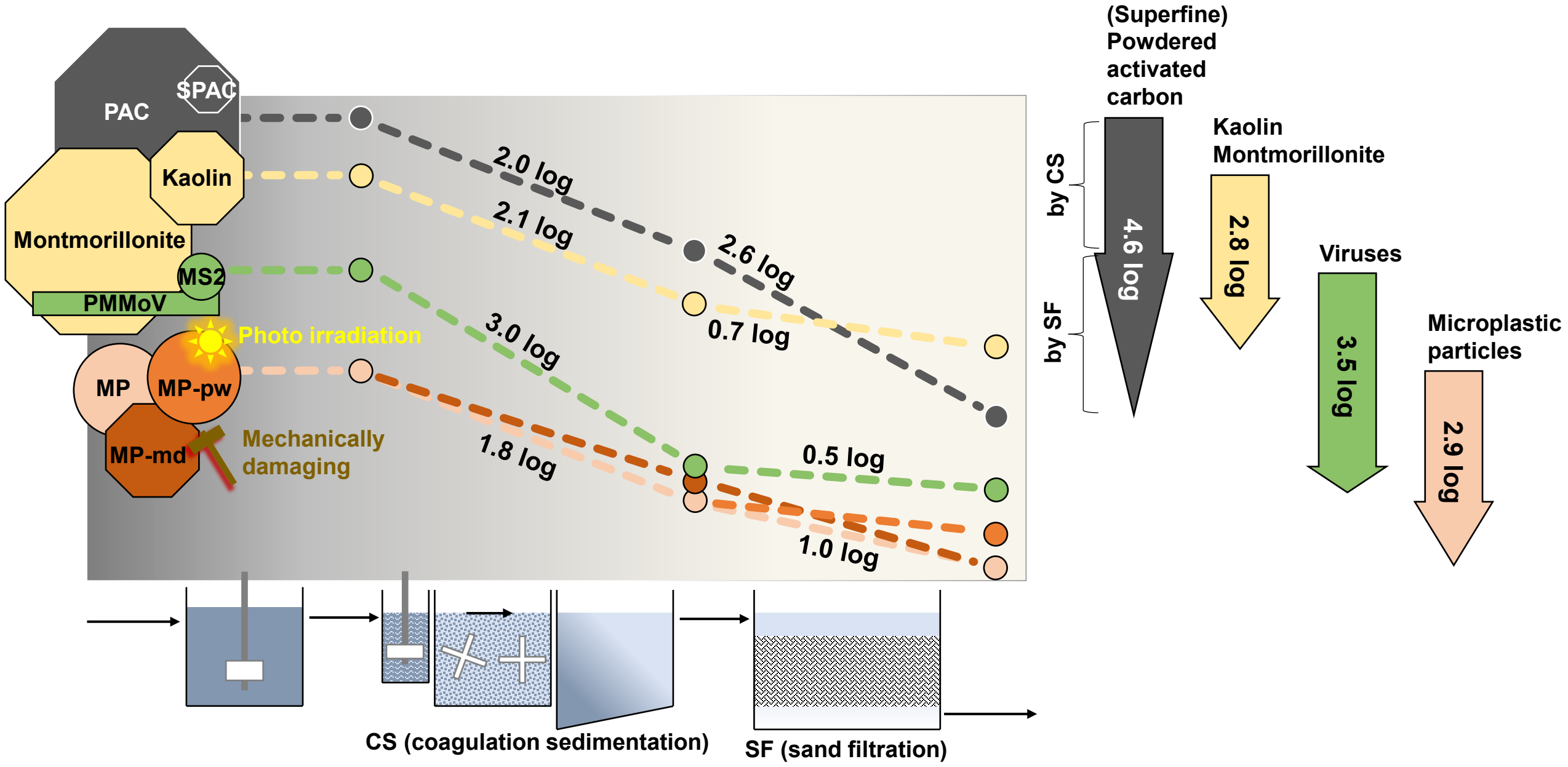
PAC
SPAC
Kaolin
Montmorillonite
MS2
PMMoV
Photo irradiation
MP
MP-pw
MP-md
Mechanically damaging
2.0 log
2.1 log
2.6 log
0.7 log
3.0 log
0.5 log
1.8 log
1.0 log
CS (coagulation sedimentation)
SF (sand filtration)
(Superfine) Powdered activated carbon
by CS
by SF
4.6 log
Kaolin Montmorillonite
2.8 log
Viruses
3.5 log
Microplastic particles
2.9 log

Supplementary Information

Differences in removal rates of virgin/decayed microplastics, viruses, activated carbon, and kaolin/montmorillonite clay particles by coagulation, flocculation, sedimentation, and rapid sand filtration during water treatment

Yoshifumi Nakazawa [a], Taketo Abe [b], Yoshihiko Matsui [c,*], Koki Shinno [b], Sakiko Kobayashi [b], Nobutaka Shirasaki [c], Taku Matsushita [c]

[a] *Department of Environmental Health, National Institute of Public Health, 2-3-6 Minami, Wako, Saitama, 351-0197, Japan*

[b] *Graduate School of Engineering, Hokkaido University, N13W8, Sapporo 060-8628, Japan*

[c] *Faculty of Engineering, Hokkaido University, N13W8, Sapporo 060-8628, Japan*

* Corresponding author: Yoshihiko Matsui, Faculty of Engineering, Hokkaido University, N13W8, Sapporo 060-8628, Japan

E-mail address: matsui@eng.hokudai.ac.jp (Y. Matsui)

Tel./fax: +81-11-706-7280

Table S1

Characteristics of raw water used in CSF tests.

Turbidity	DOC	Alkalinity	Na^+	K^+	Mg^+	Ca^{2+}	Cl^-	NO_3^-	SO_4^{2-}
NTU	mg/L	mg/L as $CaCO_3$	mg/L	mg/L	mg/L	mg/L	mg/L	mg/L	mg/L
2.7	0.8	16	12	2.1	1.8	9.7	22	1.5	20

Table S2

Experimental conditions. PA-pw indicates PA exposed to sunlight for 68 days. PA-md indicates PA mechanically damaged by ball milling. All MP particle initial concentrations were 1 μg/L, clay initial concentrations were 10 mg/L and virus initial concentrations were $10^7 - 10^8$ copies/mL.

Exp. Run No.	AC		MP	Clay	Virus	Coagulant	Figures
	type	Initial concentration (mg/L)	type	type	type	dose (mg-Al/L)	
1	SPAC	2.0	PSi	kaolin		3.0	Fig. 2, Fig. 4, Fig. 5, Fig. S6, Fig. S12
2	PAC	10	PSi	kaolin		3.0	Fig. 2, Fig. 4, Fig. S6, Fig. S8, Fig. S11
3	SPAC	2.0	PA	kaolin		3.0	Fig. 3, Fig. 4, Fig. 5, Fig. 7, Fig. S6, Fig. S7, Fig. S12
4	SPAC	2.0	PA	kaolin		3.0	Fig. 3, Fig. 4, Fig. 5, Fig. 7, Fig. S6, Fig. S7, Fig. S12
5	SPAC	2.0	PA	montmorillonite		3.0	Fig. 3, Fig. 4, Fig. S6, Fig. S7, Fig. S9
6	SPAC	2.0	PA	montmorillonite		3.0	Fig. 3, Fig. 4, Fig. S6, Fig. S7
7	SPAC	2.0	PA	kaolin		3.0	Fig. 4, Fig. S6
8	PAC	10	PA	kaolin		3.0	Fig. 4, Fig. S6, Fig. S11
9	SPAC	2.0	PA-pw	kaolin		3.0	Fig. 4, Fig. 7, Fig. S6
10	SPAC	2.0	PA-pw	kaolin		3.0	Fig. 4, Fig. 7, Fig. S6
11	PAC	10	PE	kaolin	PMMoV, MS2	3.0	Fig. 4, Fig. 6, Fig. S6, Fig. S8, Fig. S9, Fig. S11
12	PAC	10	PE	kaolin	PMMoV, MS2	3.0	Fig. 4, Fig. 6, Fig. S6, Fig. S8, Fig. S11
13	SPAC	2.0	PE	kaolin		3.0	Fig. 4, Fig. 5, Fig. S6, Fig. S12
14	SPAC	2.0	PA			1.5	Fig. 7
15	SPAC	2.0	PA			1.5	Fig. 7
16	SPAC	2.0	PA-md			1.5	Fig. 7
17	SPAC	2.0	PA-md			1.5	Fig. 7

Table S3

List of full-scale water treatment plants where sand filtrates were sampled.

Plant No	Sampling date	Raw water Turbidity (NTU)	DOC (mg/L)	PAC Material	D50 (μm)	Dosage (mg-dry/L)
1	2018/8/20	4	1.2	Wood	19	5
2	2018/8/21	2	0.6	Wood	33	3
3	2018/8/22	2	1.2	Coconut shell	17	1
4	2018/8/28	5	1.2	Wood	22	4
5	2018/8/27	7	2.2	Wood	21	14
6	2018/8/28	8	1.5	Wood	21	15
7	2018/8/24	9	2.2	Wood	22	30
8	2018/8/27	5	1.3	Wood	23	10
9	2018/9/5	14	1.4	Wood	19	10
10	2018/11/8	2	0.5	no data	5.4	1
11-1	2018/7/27	no data	0.1	Wood	21	25
11-2	2018/8/30	no data	no data	Wood	21	3
12-1	2018/8/27	4	2.5	Wood	17	15
12-2	2018/8/28	18	2.8	Wood	17	60

Plant No	Coagulant Type	Basicity %	Dosage (mg-Al/L)	Coagulation pH	Sedimentation Time (min)	Filtration Rate (m/d)	Anthracite (cm)	Sand (cm)	Time from the last backwash (min)
1	PACl	67–75	1.2	7.3	374	72	30	40	90
2	PACl	52.8	1.0	6.8	164	67	25	45	213
3	PACl	no data	1.5	6.9	85	71	no data	60	92
4	PACl	59.2	1.3	7.1	240	69	10	60	300
5	PACl	52.2	1.2	7.0	105	120	0	70	no data
6	PACl	51	2.1	6.9	170	120	0	65	540
7	PACl	49	2.9	7.0	240	120	0	80	270
8	PACl	53.1	1.4	7.0	342	120	3	60	243
9	PACl	51-55	2.1	6.9	169	83	0	65	70
10	PACl	54.7	1.1	7.3	209	no data	no data	60	360
11-1	PACl	54	1.1	7.2	47	81	7	53	no data
11-2	PACl	54	1.4	no data	47	no data	7	53	no data
12-1	PACl	51.5	1.3	7.0	139	54	0	60	35.5
12-2	PACl	51.5	2.6	7.1	156	47	0	60	24.4

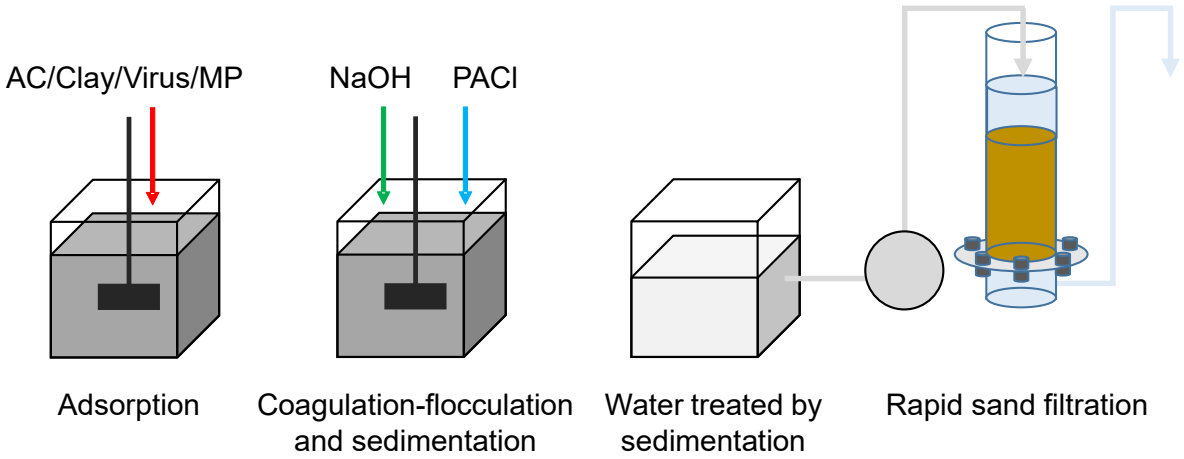

Fig. S1. Schematic diagram of the experimental setup for the coagulation-flocculation, sedimentation, and sand filtration experiment.

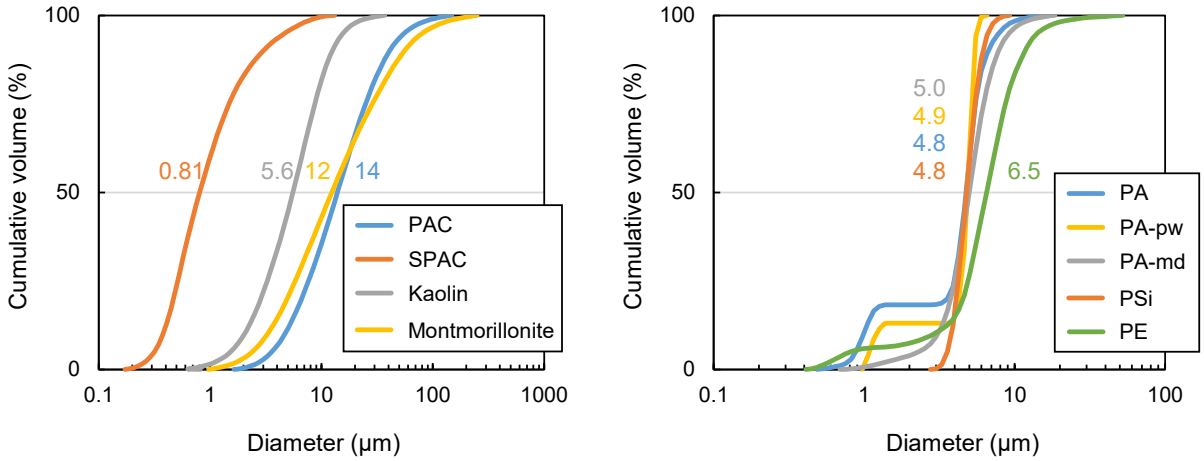

Fig. S2. Particles size distribution of PAC, SPAC, kaolin, montmorillonite, PA, PA-pw, PA-md, PSi, and PE. The numbers indicate D50 (volume median diameter) of particles associated with lines of the same color.

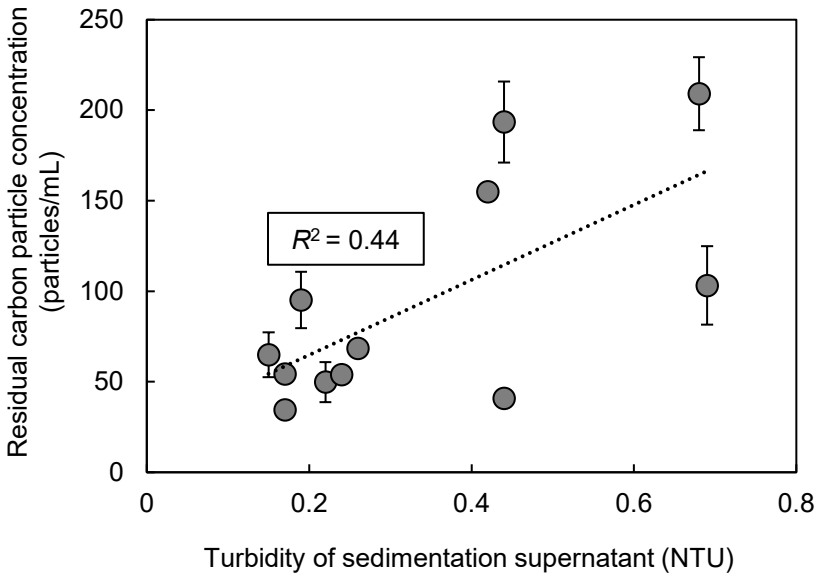

Fig. S3. Regression between the residual carbon particle concentrations and the turbidities of settled waters. The data were obtained from all of the 14 full-scale water purification plants using CSF processes. The dotted line indicates the regression line. Error bars indicate standard deviations of three measurements, but some of them are hidden behind the symbols.

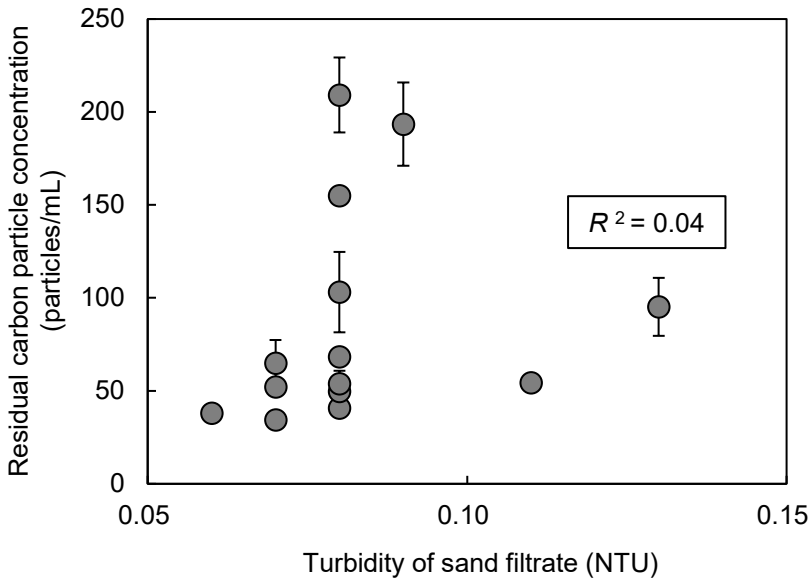

Fig. S4. Correlation between the residual carbon particle concentrations and turbidities of sand filtrate. The data were obtained from all of the 14 full-scale water purification plants using CSF processes. Error bars indicate standard deviations of three measurements, but some of them are hidden behind the symbols.

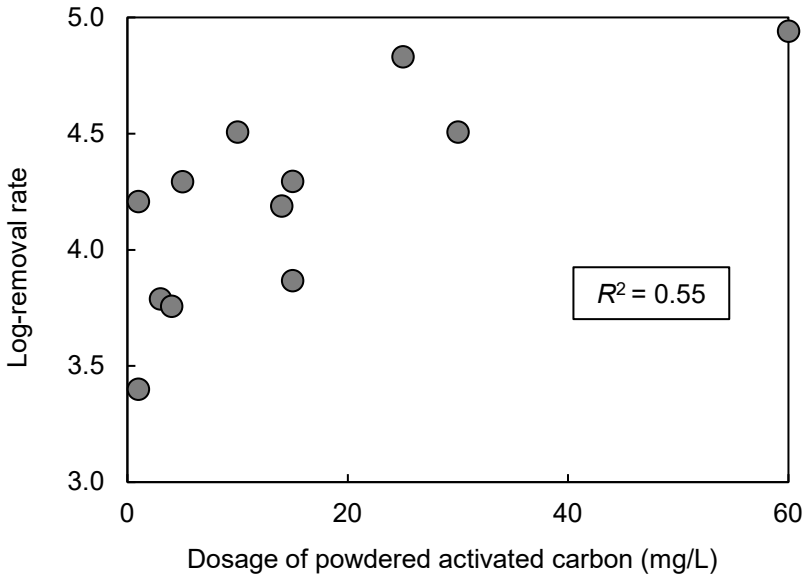

Fig. S5. Correlation between the log-removal rate of carbon particles and the dosage of powdered activated carbon. The data were obtained from the 12 full-scale water purification plants using CSF processes. Two initial carbon particle concentrations of the plants could not obtain and so are excepted.

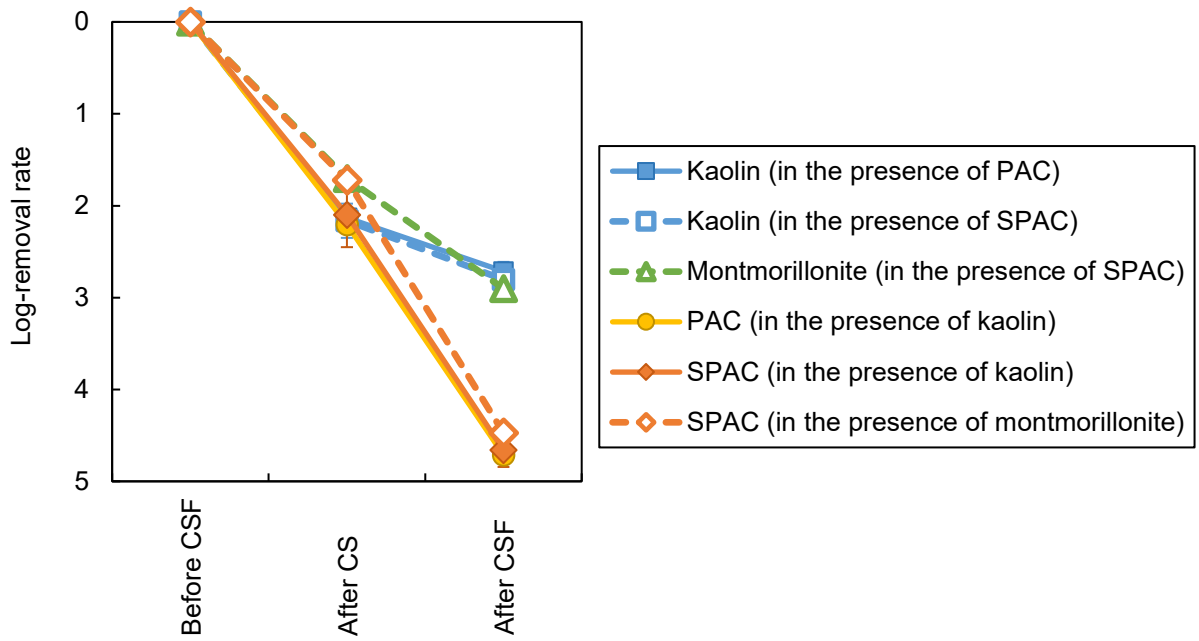

Fig. S6. Log-removal rate comparison between kaolin, montmorillonite, PAC, and SPAC during the CSF process. The data are also listed in Table 1. Data from Runs 1, 2, 3, 4, 5, 6, 7, 8, 9, 10, 11, 12, and 13. Details of the experimental conditions are presented in Table S2. Error bars indicate standard deviations of experiments, but some of them are hidden behind the symbols.

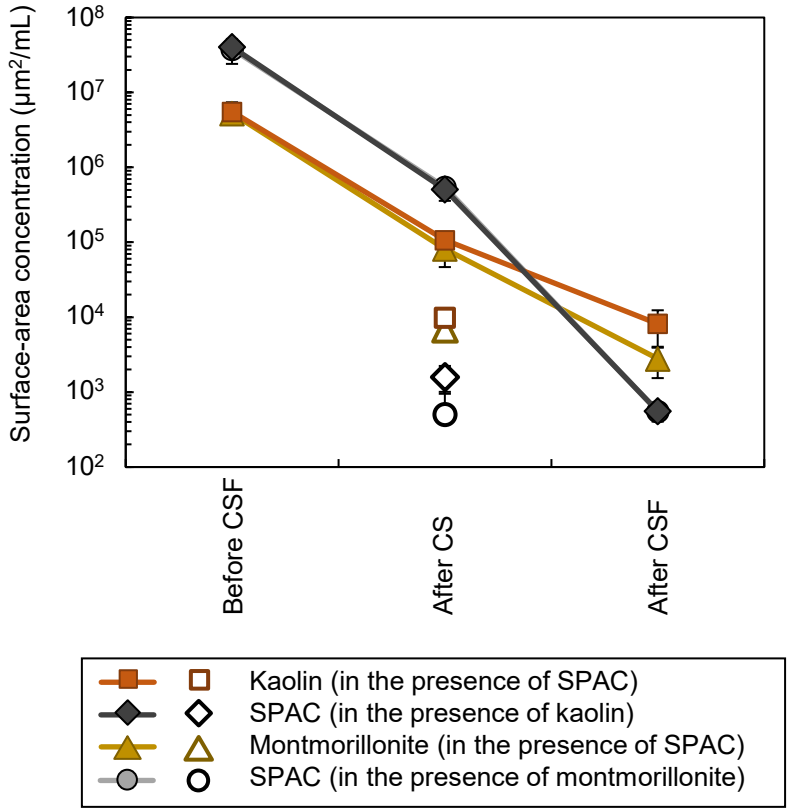

Fig. S7. Comparison of removal rates by CSF between kaolin, montmorillonite, and SPAC quantified in terms of surface-area concentrations. Either kaolin or montmorillonite and SPAC were added simultaneously. The open symbols indicate the data measured after centrifugation. Data from Runs 3, 4, 5, and 6. Details of the experimental conditions are presented in Table S2. Error bars indicate standard deviations of experiments, but some of them are hidden behind the symbols.

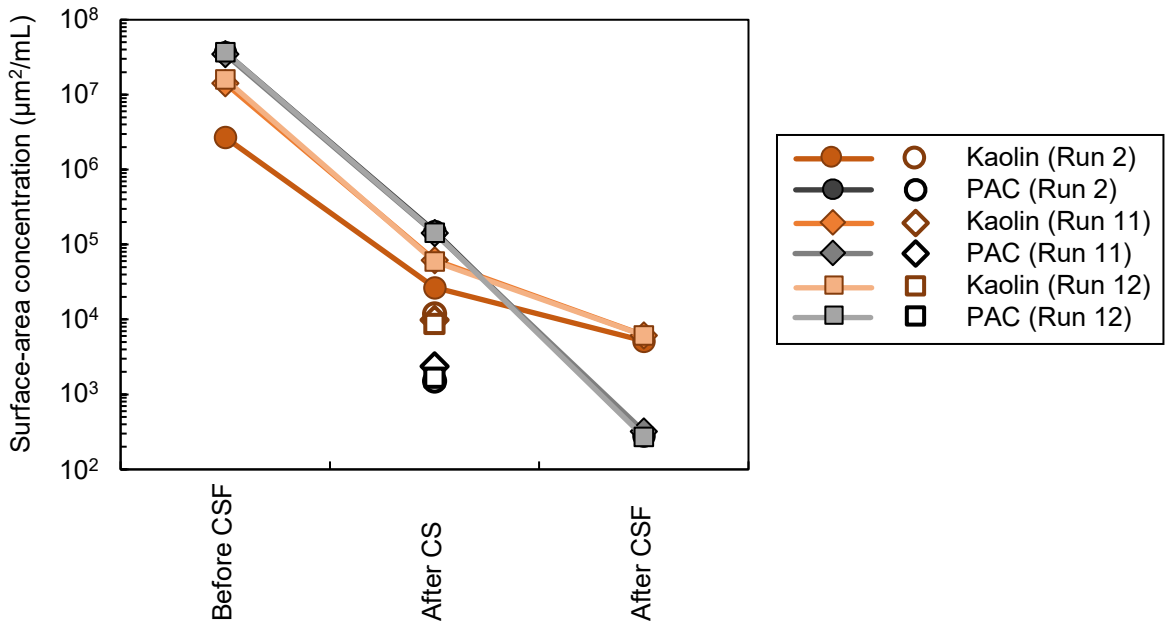

Fig. S8. Comparison of removal rates by CSF between kaolin and PAC quantified in terms of surface-area concentrations. Kaolin and PAC were added simultaneously. The open symbols indicate the data measured after centrifugation. Data from Runs 2, 11, and 12. Details of the experimental conditions are presented in Table S2.

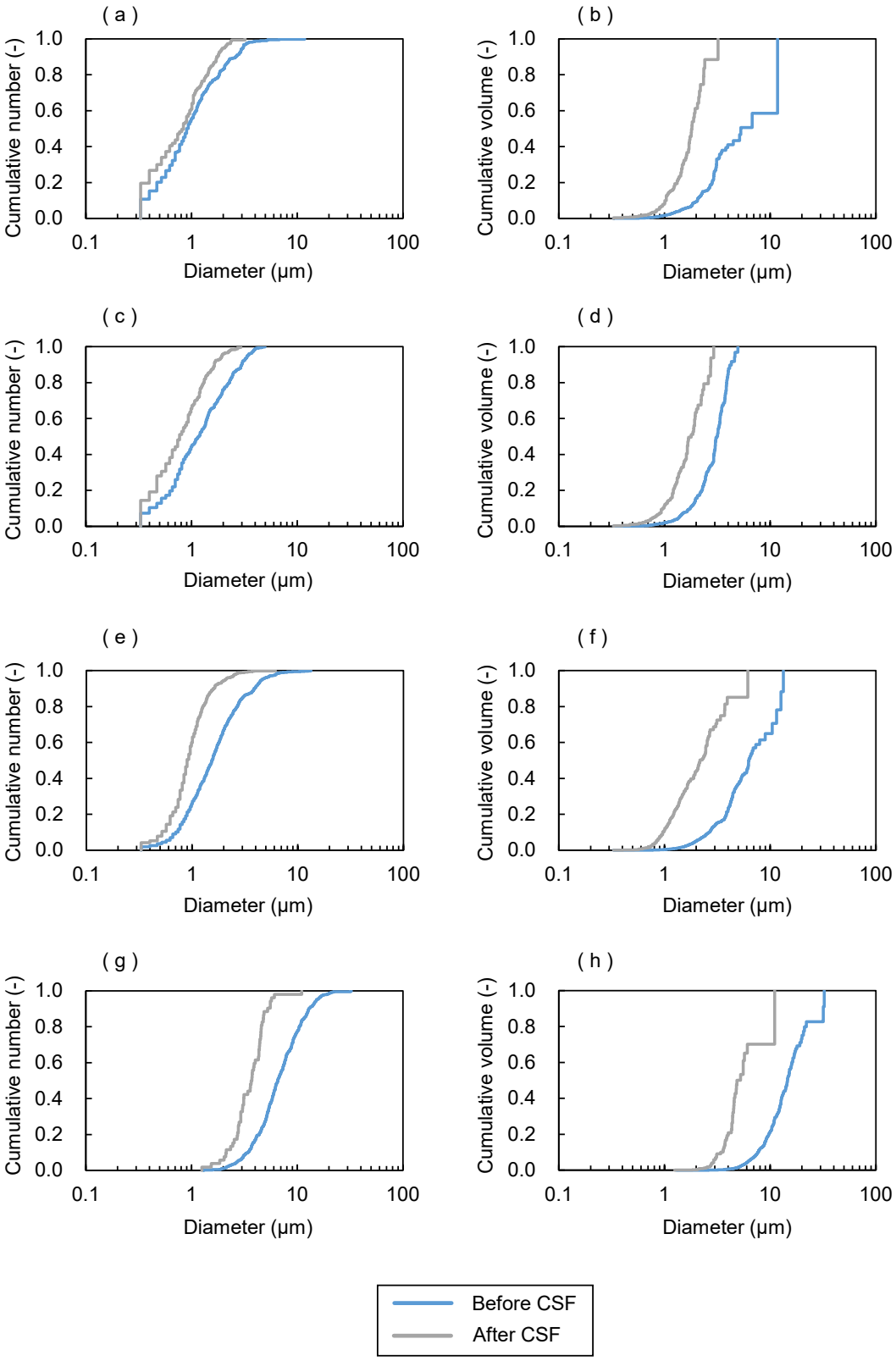

Fig. S9. Particles size distribution of PAC, SPAC, kaolin, and montmorillonite before and after the CSF process. Panels a and b: PAC. Panels c and d: SPAC. Panels e and f: kaolin. Panels g and h: montmorillonite. Panels a, c, e, and g: cumulative numbers. Panels b, d, f, and h: cumulative volumes. Data from Runs 5 and 11. Details of the experimental conditions are presented in Table S2.

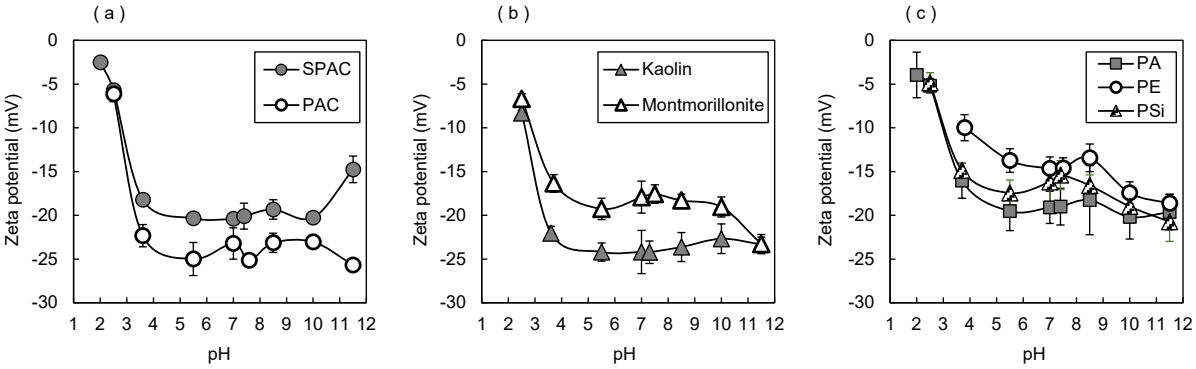

Fig. S10. Comparison of zeta potential between particles. Panel a: activated carbon particles. Panel b: clay particles. Panel c: MP particles. Error bars indicate standard deviations of measurements, but some of them are hidden behind the symbols.

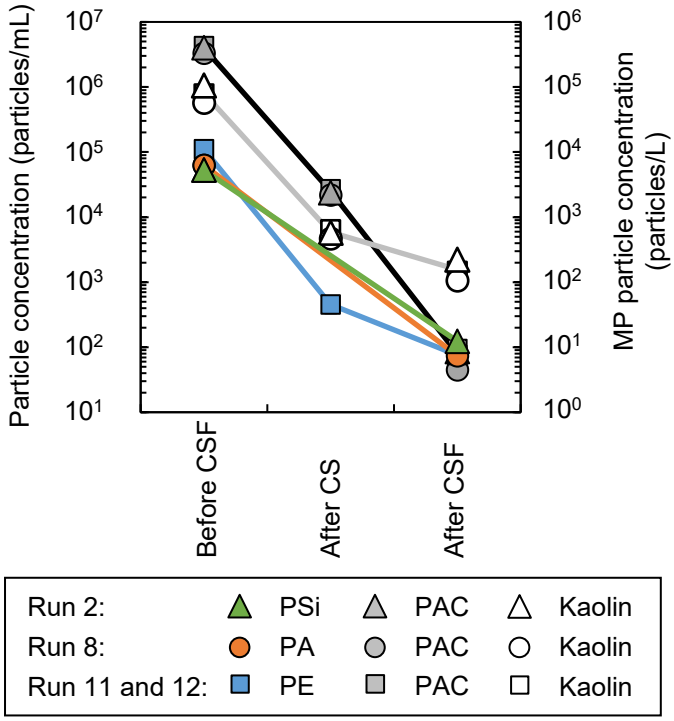

Fig. S11. Behavior of PE, PA, and PSi during the CSF process. PA, PSi, and PE were each treated by CSF in the presence of PAC and kaolin. Data from Runs 2, 8, 11, and 12. Details of the experimental conditions are presented in Table S2. Error bars indicate standard deviations of experiments, but some of them are hidden behind the symbols.

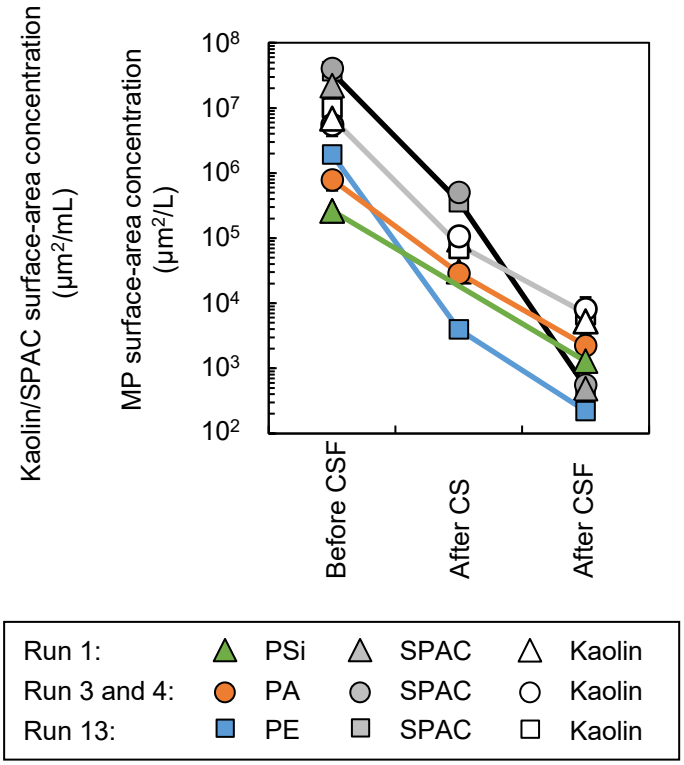

Fig. S12. Behavior of PE, PA, and PSi during the CSF process. PA, Psi, and PE were each treated by CSF in the presence of SPAC and kaolin. Data from Runs 1, 3, 4, and 13. Details of the experimental conditions are presented in Table S2. Error bars indicate standard deviations of experiments, but some of them are hidden behind the symbols.

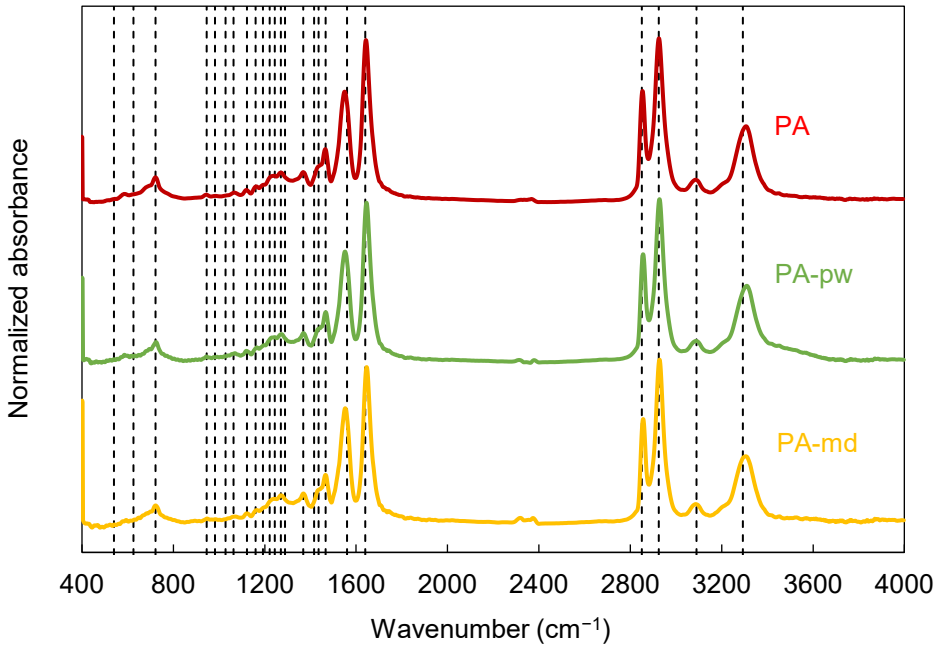

Fig. S13. FTIR of PA particles before and after weathering.

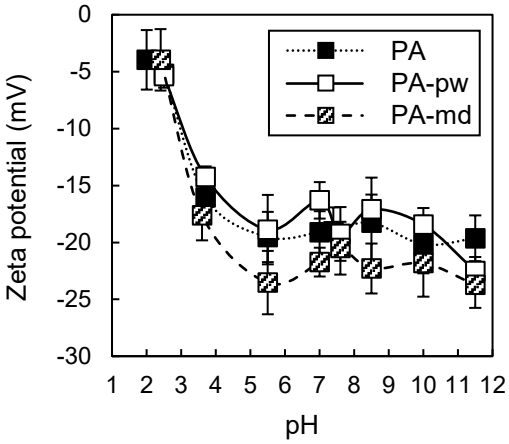

Fig. S14. Zeta potential of PA particles before and after weathering. PA-pw stands for PA exposed to sunlight for 68 days. PA-md stands for PA mechanically damaged by ball milling. Error bars indicate standard deviations of measurements, but some of them are hidden behind the symbols.